Dissolution Phenomenon of Some Optical Glass in an Acid

By Shoji TSUCHIHASHI

(Received April 2, 1949)

Introduction

Many studies have been made concerning the effect of acid on optical glass from the standpoint of the scientific research or the practical use. There are numerous reports[1,2,3,4,5] on the relation between the amount of the alkali dissolved and the time of dissolution. In most of these experiments powdered glass was used and the alkali dissolved in an acid solution after immersing the sample in it was titrated. In such cases, as pointed out by Tieze[1], it happens frequently that the metal ions present near the surface may dissolve at first without being peeled off of the SiO_2 film formed on the surface sloughs, therefore the reaction velocity is hard to measure.

The author adopted the method of measuring the apparent velocity through the change of interference color which was caused by the thickness of the SiO_2 film formed after the escape of metal ions from glass. In this method the SiO_2 film is not peeled off, so it is very advantageous to the observation of the erosive action of an acid for the polished surface of glass.

Experimental Method

The apparatus is shown in Fig. 1. A polished sample of optical glass, b, supported by a Terex

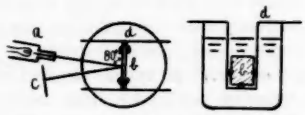

Fig. 1.—Experimental apparatus.

glass holder, d, was washed with alcohol, immersed for 1 minute in a 0.5 *N* solution of caustic soda, and washed again thoroughly with distilled water. Immediately after this treatment, it was immersed in a nitric acid solution kept at a constant temperature. After that, with much attention to the change of the temperature, the reflection of the light radiated from the light source, a, was caught on a screen, c, and the change of the interference color with the time was observed at a desired temperature.

The change thus observed was examined from the relation between the interference color in the case of Newton's ring and the thickness of a film (SiO_2 film; $n=1.46$), and graphically shown in Fig. 2 as the relation between the thickness of a film and the time. A number of plates ($24\times20\times2$ mm. in size) of Flint glass (F-1, F-2, F-3, SF-2, KF-2 glass) were examined, each of which has been cut from the lump glass and polished under the same condition.

Their components are shown in Table 1.

Table 1

Composition of Glass

Glass	Component, %					
	SiO_2	PbO	Na_2O	K_2O	Al_2O_3	ZnO
F-1	45.0	45.1	1.5	7.7		
F-2	44.7	46.2	0.2	8.8	0.02	
F-3	45.6	43.4	1.7	8.6		
SF-2	40.99	51.1	0.6	6.9	0.04	
KF-2	66.8	11.6	16.0	0.1	1.5	3.8

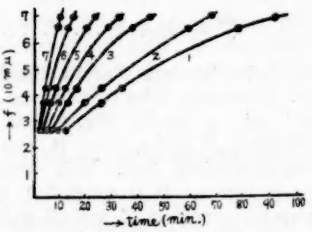

Fig. 2.—*f-t* curve of the F-2 glass: 1, 60°C.; 2, 63°C.; 3, 66.5°C.; 4, 70°C.; 5, 75°C.; 6, 80°C.; 7, 84.5°C.

Experimental Results and Discussion

(1) On the Concentration Change of the Acid through the Experiment.—The change of the concentration of the 1 *N* nitric acid was examined by the volumetric analysis, and it was almost negligible for the present investigation.

(2) On the Reaction Velocity.— When

(1) P. Tieze, *Sprechsaal*, **61**, 809 (1928); *Glastech. Ber.*, **6**, 716 (1928-29).
(2) G. Keppeler, *Glastech. Ber.*, **12**, 366 (1934); *Chem. Centr. Bl.*, 2026 (1935).
(3) E. Berger, *Glastech. Ber.*, **14**, 351 (1936); **16**, 296 (1938).
(4) T. Moriya, *J. Soc. Chem. Ind. Japan*, **43**, 884, 886 (1940).
(5) S. Nagaeda, *J. Japan. Cer. Assoc.*, **49**, 140 (1941).

CHEMISTRY HALL LIBRARY

optical glass is immersed in an acid, the reflection from its surface gradually changes. This is ascribed to the formation of a film on the glass surface which differs from the base glass in the index of refraction and the film formed is a SiO_2 film, as clearly known from the studies of Blodgett and others[6,7,8], so the refractive index of the film is considered to be 1.46.

In the case of ordinary soda-lime glass, the immersion in an acid solution does not cause the variation in the interference color, but alkali is dissolved in the solution. In the case of KF-2 glass, after showing a certain interference color, it becomes colorless. This indicates that the film remains without being peeled off to a certain thickness and then all was peeled off. In the case of F-2 glass, the interference color was gradually changed, which indicates that the SiO_2 film is not removed.

Therefore, it is phenomenologically inferred that PbO and K_2O present in the glass, reacting with nitric acid to be $Pb(NO_3)_2$ and KNO_3, are removed and then the skeleton of SiO_2 remains with the water included.

The relation between the amount of reaction and time, as shown in Fig. 2, is generally parabolic. If the diffusion of something is supposed to be the factor for this reaction, the following equation is to be established.

$$\frac{df}{dt} = k\frac{1}{f} \quad \cdots\cdots\cdots\cdots (1)$$

where f is the thickness of the film. By integrating equation (1), it becomes (2),

$$f^2 = 2kt + k' \quad \cdots\cdots\cdots\cdots (2)$$

and the relation between f^2 and t (time) should be linear. From this point of view, the relation between f and t given in Fig. 2 was revised as that between f^2 and t, then it was represented as a straight line. This justifies the above presumption. It is concluded that the dissolution phenomenon of optical glass in an acid is parabolic at its initial stage, and its reaction velocity is dominated by the diffusion of some substance.

In Fig. 3 the relation between the reaction velocity k and the temperature is shown; the relation $\log k$ and $1/T$ is linear and there holds the following equation:

$$K = Ae^{-\frac{E}{RT}} \quad \cdots\cdots\cdots\cdots (3)$$

This may properly show that the reaction velocity is dominated with the diffusion of some substance.

(3) Influence of the Additive Ion in the Solution.—It is considered possible that the escaped ions from the glass may have some influence on the formation of this film.[9,10] For the purpose of full discussion, we have traced the influence of the K^+ Pb^{++} on the SF-2 glass in the nitric acid. We have adopted the 100 cc. solution of 1 N nitric acid, in which 0.1 mg., 0.5 mg., 1 mg., 5 mg., 10 mg. of KNO_3 and $Pb(NO_3)_2$ were dissolved respectively at 50° and 80°.

It may be concluded from this experiment that the K^+, Pb^{++} in the nitric acid give no influence on the reaction velocity described above.

(4) Influence of Stirring on the Dissolution.—When the solid dissolves in the liquid, it is well-known fact that the diffused layer, formed between the rubbing faces of the solid and the liquid, is very strong and does not come off easily, and that the diffusion of the ions or others through this layer generally determines the reaction velocity.

Dissolution phenomenon of the optical glass in an acid is not considered so simple as above mentioned, but it may be considered to contain that this phenomenon is found in one part of the diffused systems, then the possible existence of the diffused layer may be taken up for consideration.

For experimental convenience the author did not circulate the solution, on the other hand shaked up and down the test pieces of the optical glass (SF-2) in the solution. The distance of the movement in the solution was about 6 cm., and the number of times to move up and down 90 to 100 for one minute.

The observation of the reaction velocity was made by the optical method as similar to that mentioned above. The results showed that the reaction velocity becomes a little faster by the stirring but its amount is so small that the stirring gives no influence on the reaction velocity.

As it is unnecessary to consider the diffused layer which exists at the boundary between glass and liquid, it may be concluded that the diffusion which determines the reaction velocity is in the glass itself.

(5) On the Peculiarity of the SiO_2 Film.—As mentioned above, the author adopted

(6) K. B. Blodgett, *Phys. Rev.*, **55**, 391 (1939).
(7) I. Sawai, J. Tashiro and K. Umeya, *J. Japan. Cer. Assoc.*, **52**, 109, 198, 200 (1944).
(8) I. Sawai, J. Tashiro, K. Umeya, and S. Kozaki, *J. Japan. Cer. Assoc.*, **52**, 258 (1944).
(9) Geffeker, *Kolloid Z.*, **86**, 11 (1939).
(10) D. Hubbard and F. H. Hamilton, *J. Res. Nat. Bur. Stands.*, **27**, 143 (1941).

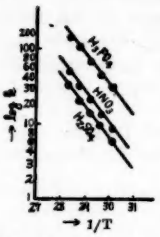

Fig. 3.—SF-2 glass.

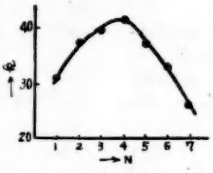

Fig. 4.—F-2 glass at 80°C.

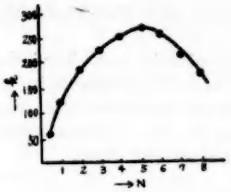

Fig. 5.—SF-2 glass at 80°C.

the method of measuring the apparent velocity through the change of interference color.

It means the safe existence of the skeleton of the SiO_2 retaining the binding force by hydrogen ions or water molecules which got into the hole formed after the escape of metal ions. The phenomenon in proof of this fact is that the interference color glides off into the one which is produced when the film seems to have decreased in thickness, if the glass is taken out into the air and decomposed by heat.[11]

It is considered that the water included in SiO_2 skeleton run out by the the heat treatment and the film shrinks a little. In the case of KF-2 glass mentioned above, the intimate relations might be thought to exist between the inner constitution of the glass and the thickness of SiO_2 film capable of maintaing the SiO_2 linkage.

So it is surmised that the SiO_2 film is not peeled off but stays on the glass surface at the Flint glass, but the binding force acts in various ways in relation to the change of the glass component and inner constitution.

The author considered that the refractive index of the film is uniformly 1.46. But Schröder[12] reported that the erosive film has not a simple refractive index as fused quarts, but some gradient along the depth of the film. He also reported that it has no objection to use the average refractive index $\bar{n}$. (actually it is a serious question what value is to be used for n.)

When the initial stage of these reactions come into question, *i. e.*, the film is very thin, it may be considered that as if Na^+, K^+, Pb^{++} etc. are stayed in the SiO_2 film, and refractive index of the film grows larger corresponding to go into the inner part of the film. But this difference is very small, and it has no objection to think the refractive index of the film is almost 1.46.

(6) Experiment in the Sulfuric Acid and Phosphoric Acid.—The initial dissolution phenomenon in an acid with 1 *N* sulfuric acid and 1 *N* phosphoric acid besides 1 *N* nitric acid was studied, and it is found to proceed parabolically.

Fig. 3 shows the relation between $\log k$ and $1/T$ in the case of SF-2 glass. These linear lines only get loose in parallel and it is considered that the rate determining stage of this reaction is not caused by the diffusion of the anions (NO_3^-, SO_4^{--}, PO_4^{---}) in the glass.

(7) The Relation between the Reaction Velocity Constant and the Concentration of the Solution.—In the curve expressing the relation between the reaction velocity constant and the initial concentration of the solution there appears a maximum point in Fig. 4 and Fig. 5 in the case of F-2 and SF-2 glass and the position of the maximum points in two curves are not coincident.

This disparity of the maximum points is due to the amount of PbO contained in each optical glass, so it is considered that for the rate determining stage of this reaction the amount of PbO in the glass play an important part.

Conclusion (Reaction Mechanism)

It is surmised from the facts mentioned above that the mechanism of these reactions is as follows.

At first Na^+, K^+ and Pb^{++} that existed combined with the tetrahedron of the SiO_2 in the glass are brought out, *i. e.*, diffused to the glass surface and thrown up into the solution leaving holes. Thus the skeleton layer of SiO_2 is formed. Then H^+, H_3O^+ etc. enter into the holes of the skeleton layer and Na^+, K^+ and Pb^{++} are diffused out further from the more inner part of the glass for the lack of the positive charge.

It is considered that the reaction is advanced by these courses, and that, therefore these reactions are the exchange reaction between

(11) S. Tsuchihashi, unpublished.
(12) H. Schröder, *Ann. Phys.* **39**, 55 (1941).

Na^+, K^+, Pb^{++} and H^+, H_3O^+.

As mentioned above, the diffusion of the Pb^{++} carry out the important role in these steps.

It may also be considered that this mechanism is not unreasonable in consideration of the relation between the reaction velocity constant k (or diffused constant) and the component of the glass.

In conclusion the author wishes to express his thanks to the director of this institute Dr. K. Fuwa, and also to Professor S. Horiba (Kyoto University) for their stimulating interest in the author's work.

Research Institute,
Tokyo Shibaura Electric Co. Ltd., Kawasaki

Pyrolysis and Combustion of Cellulose in the Presence of Inorganic Salts

By Kenzi TAMARU

(Received March 2, 1951)

Introduction

Some chemicals which when applied to cellulose inhibit flaming of gases or combustion charcoal are called fire-resisting compounds, and several of them are, for example, ammonium sulphate and phosphate, aluminium sulphate and zinc chloride. Many investigations have been made on the action of the compounds since olden times.[1]~[6]

The present author has studied on the process of carbonization of cellulose in the previous paper[7] and reached the following conclusion. Generally speaking, by the carbonization of cellulose, charcoal is not produced by the continued collapse of cellulose structure, but the high molecules of cellulose are first depolymerised to low molecules by heat, a part of which evaporates increasingly as the rate of heat increases and the other part, being dehydrated, polymerizes to yield a high polymer, direct origin of charcoal. This polymer is degassed by heat, being cut its weak bindings and proceeding aromatization side by side in the structure. Such gases as carbon dioxide, carbon monoxide, methane or hydrogen are evolved from it, consequently producing the "molecular roughness" or "Ultraporosität" in it. By further heating the gas evolution and the aromatization proceed and the "molecular roughness" increases till about 800°. However, it begins, in turn, to be eliminated by gradual breaking down of the skeleton of the polymer structure over 1000°, and by the severe treatment of heat the graphitization proceeds.

In the presence of some chemicals the process of carbonization of cellulosse being affected, the change in flammability of cellulose in this case is possibly attributed to that in carbonization process.

In this paper, the carbonization and combustibility of cellulose in the presence of various salts are reported to consider the action of fire-resisting compounds.

Experimental

Effect of Inorganic Salts on the Pyrolysis of Cellulose:—The sample[8] was treated in the 0.1 mol. solutions of various salts. About 0.5 g. of dry sample was put in the bottom of the quartz tube which was closed at one end. The tube was connected to a gas burette. After evacuating the air from the tube and the burette, the sample was thermally decomposed by inserting the bottom of the tube perpendicularly in an electric heater, the temperature of which was 480°. The gas evolved by the decomposition of the sample was conducted to the gas burette and after being heated for an hour, the gas was

(1) Gay Lussac, *Ann. chim. phys.*, **18**, 211 (1821).
(2) S. Tamaru, Y. Imai and T. Momma, *J. Chem. Soc. Japan*, **55**, 30 (1934).
(3) N. A. Richardson, *Chem. and Ind.*, **56**, 202 T (1937).
(4) R. W. Little, *American Chemical Society Monograph* No. 104 (1947).
(5) K. Tamaru, *J. Chem. Soc. Japan*, **69**, 20 (1948).
(6) American Chemical Society Symposium on "Flame Retarding of Textiles," *Ind. Eng. Chem.*, March, 1950.
(7) K. Tamaru, *J. Chem. Soc. Japan*, **69**, 21 (1948).

(8) Toyo Filter Paper No. 41, which contains no inorganic salt, was used as the sample.

Table 1

Salt	Total gas volume, cc./g.	CO_2, %	CO, %	CH_4, %	H_2, %	Others, %	R_1, %	R_2, %	V, %
Without salt	144	48	34	17	0	1	6	31	24
H_3BO_3	120	44	43	11	2	1	13	20	33
NH_4Cl	101	44	31	15	8	2	29	2	51
$(NH_4)_2SO_4$	132	45	35	19	0	0	33	0	66
$(NH_4)_2HPO_4$	89	42	43	9	2	4	39	0	79
NH_4-molibdate	148	51	29	14	6	0	34	4	57
$(NH_4)_2PtCl_6$	149	42	24	18	17	0	—	9	45
LiCl	151	49	29	18	0	5	25	13	61
KCl	178	45	32	21	0	2	29	11	60
KBr	128	53	26	16	1	3	24	17	57
KI	109	53	23	15	7	3	28	18	56
$KClO_3$	155	48	35	13	3	1	17	22	62
K_2SO_4	192	44	29	25	0	2	19	19	50
KNO_3	239	45	29	16	11	0	29	5	71
KH_2PO_4	123	46	39	15	0	0	31	10	58
K_2CO_3	242	42	23	26	6	3	31	1	75
KCN	234	42	33	25	0	0	35	0	76
KCNS	237	43	29	21	6	2	30	0	73
$K_4Fe(CN)_6$	266	38	23	15	24	0	55	1	71
$K_3Fe(CN)_6$	276	40	20	14	25	0	47	0	69
K_2SiO_3	234	43	30	22	4	2	35	0	78
$K_2Cr_2O_7$	240	49	16	23	10	3	39	0	55
NaOH	223	46	34	20	0	0	28	1	79
NaCl	165	50	28	20	0	2	20	12	56
Na_2SO_4	177	46	34	18	0	1	18	17	45
$Na_2S_2O_3$	219	51	32	17	0	0	31	0	84
Na_2CO_3	210	45	36	19	0	1	29	1	82
$Na_2B_4O_7$	132	51	32	16	1	1	43	3	73
$MgCl_2$	124	50	32	16	0	1	28	2	59
$CaCl_2$	143	54	22	21	2	3	42	2	62
$BaCl_2$	128	51	31	17	0	1	20	15	49
$AlCl_3$	129	43	40	17	0	1	22	14	41
$Al_2(SO_4)_3$	140	46	43	8	2	1	39	1	76
Rb-alum	146	51	33	14	1	1	21	13	47
$CrCl_3$	146	45	29	16	9	2	29	9	57
$MnCl_2$	124	49	32	15	3	2	32	7	47
$MnSO_4$	164	49	31	15	5	1	21	18	34
$FeCl_2$	90	48	32	12	6	2	18	23	53
$FeSO_4$	146	52	26	15	6	2	27	9	52
$FeCl_3$	118	46	28	13	11	3	33	5	69
$CoCl_2$	120	29	37	15	15	4	45	2	65
$NiCl_2$	161	33	32	16	16	4	29	12	49
$CuCl_2$	118	42	32	13	12	2	20	17	54
$CuSO_4$	158	45	35	13	7	0	26	10	66
$AgNO_3$	179	47	28	11	13	1	16	23	48
$ZnSO_4$	146	43	37	7	12	1	25	6	51
$CdCl_2$	143	43	16	15	20	6	31	8	56
HgCl	70	49	37	10	4	1	17	21	46
$HgCl_2$	92	46	35	13	4	2	14	31	39
HgI_2	46	49	36	10	5	1	14	46	48
$SnCl_2$	151	41	21	11	24	2	41	2	55
Pb-acetate	214	46	25	21	8	1	34	1	41
$PdCl_2$	218	25	46	15	13	1	16	24	78
$CuSO_4$*	131	52	35	8	3	2	—	—	62
$CuSO_4$**	154	45	35	14	6	1	35	2	—

* The experiment was carried out at 430°.
** The experiment was carried out under the pressure of one atmosphere of carbon dioxide.

Table 2

The Effect of Inorganic Salts on the Combustion of Cellulose (1)

Salt	t, sec*.	Height of flame, cm.
Without Salt	35.0	3.2
H_3BO_3	31.6	2.6
NH_4Cl**	35.0	2.7
$(NH_4)_2HPO_4$**	35.8	2.2
$(NH_4)_2SO_4$**	40.3	1.8
LiCl	33.7	2.8
KCl	28.8	3.4
KBr	26.4	4.2
KI	24.7	5.0
$KClO_3$	20.2	4.8
K_2SO_4	38.7	2.6
KNO_3	29.8	2.4
KH_2PO_4**	47.3	1.3
KCNS	38.0	2.1
Na_2SO_4	38.1	2.4
$NaHSO_4$	25.1	4.2
$Ca(OH)_2$	37.7	2.8
$BaCl_2$	29.3	3.4
$MnSO_4$	25.1	3.3
$FeSO_4$	28.3	2.6
$CuCl_2$	31.2	4.2
$CuSO_4$	35.3	2.1
$ZnSO_4$**	26.3	3.3
$CdCl_2$**	28.5	3.0
$HgCl_2$	30.7	3.3
Pb-acetate	37.7	2.4

* The time taken to spread the flame in the middle 12 cm. length of the sample.

** The sample remained as charcoal as it was after the flame had passed over.

pumped out and then analysed. Carbon dioxide, carbon monoxide and heavy hydrocarbons were determined by absorbing with potassium hydroxide solution, cuprous chloride solution and fuming sulphuric acid, respectively and after the removal of the above gases, hydrogen and methane were estimated by the explosion method.

The results are shown in Table 1. R_1 in the table denotes the charcoal yield and V_1 the approximate percentage of the gas evolved in the first three minutes and it shows the rough decomposition velocity. Organic vapour produced by the decomposition was condensed at the upper part of the tube out of the heater, then the liquid produced went down along the tube and carbonized at the entrance of the heater. The amount of chars thus produced is designated by R_2 in the table.

Effect of Inorganic Salts on the Combustion of Cellulose:—The effect of inorganic salts on the combustion of cellulose was measured by burning the filter paper which was treated by 0.1 mol solution of various salts. The sample was supported its both sides by the folded sheets of glass plates respectively and was placed in such a way that the glass plates were parallel with the width of 1.5 cm.(9) and its gradient was 1/7 to horizon. The sample was ignited at its lower end and the time taken to spread the flame 12 cm. length in the middle was measured. The height of the flame was also measured using a perpendicular graduated mirror. Every experiment was carried out under the same condition as possible and the results were obtained by taking an average of the repeated experiments.

The results are shown in Table 2. The samples treated by such salts as potassium carbonate, silicate, bichromate and ferrocyanide, borax, $Na_2S_2O_3$ and alminium sulphate were non-flammable and when the sample was horizontally placed those of ammonium sulphate and phosphate were also incombustible.

Consideration

We will see in Table 1 that by the presence of inorganic salts, R_1 was increased, R_2 decreased, while the velocity of decomposition became faster.

The volume of the gas produced was much affected by the inorganic salts. For example, in the experiment of mercuric iodide it was 46 cc./(g. cellulose) and of potassium ferricyanide 276 cc./(g. cellulose). The former was approximately one third of that of the untreated cellulose and the latter, about two times of it. The volume of the gas was increased by palladium and alkaline salts and decreased by mercuric or mercurous salts. The alkaline salts increased the volume of the gas in the following order: lithium, sodium, potassium and rubidium salts. The difference of valency showed a different effect as shown in the case of Fe salts. As for the anions, the volume of the gas was increased by carbonate, hydroxide, cyanide, ferri- and ferrocyanides and nitrate. Moreover, among sulphate, chloride, bromide and iodide, the relation that, if the cation present is the same, the volume of the gas became smaller in the order described above was found out.

As to the composition of the gas, it did not show so much effect of the compounds, that is, about 45 to 50% was carbon dioxide and ts 30% was carbon monoxide and the major part of the remainder was methane. But most salts of the transition metals showed an increased content of hydrogen relative to oxygen in the gas.

When the pyrolysis was carried out in the atmosphere of carbon dioxide, the result was approximately the same, except the increased

(9) If a larger width was taken the flame became higher and the velocity of combustion larger.

value of R_1 and decreased R_2. This showed that the evaporation of the organic vapour was suppressed by the presence of carbon dioxide and that the gaseous products by the carbonization of the organic vapour and those of the cellulose were not so different in this case.

At the lower decomposition temperature, the volume of the gas was decreased and its composition became richer in oxygen, showing that oxygen was more easily decomposed than hydrogen by the carbonization.

As to the results of the combustion experiment, it will be seen in Table 2 that higher the flame, faster the combustion velocity, and the velocities in the order of decreasing rates were: iodide, bromide, chloride and sulphate.

Oxidizing agents, such as potassium nitrate and chlorate, showed a faster velocity of combustion. The effect of the hydrated water on the salts was not directly observed.

T. Tatibana[10] studied on the effect of the inorganic compounds on the ignition temperature of cellulose. He measured the lowest temperature enough to set cellulose, which was treated by inorganic salts, on fire, when the sample was put in the furnace. The "ignition temperature," which he so called, corresponds to the temperature at which the sample begins to ignite without flame, and the "flaming temperature," to fire with flame.

H. Akamatu and H. Hamada[11] measured the effect of the various inorganic salts on the ignition temperature of carbon black[12], which contanied 5% salts in it using a simple thermobalance. The results are shown in Table 3.

Now we come to consider the action of fire-proofing compouuds, referring to the abovementioned data. Some investigators suggested[2] that the action of fire-roofing compounds is possibly to let the valume of the combustible gas evolved by the pyrolysis to decrease and render cellulose noninflammable. However, though potassium carbonate, for instance, showed a large increase in the amount of combustible gas and, more over, the velocity of pyrolysis was large, it is practically one of the fire-resisting compounds. On the other hand, mercuric chloride showed only a small amount of combustible gas and had a slow decomposition velocity and, nevertheless, it is'not a fire-resisting compound.

This contrast shows that the fire-resisting action is not mainly responsible to the amount

Table 3

The Effect of Inorganic Salts on the Ignition Temperature of Carbon Black

Salt	Ignition temp., °C.	Salt	Ignition temp., °C.
Without salt	491	Rochelle salt	359
LiCl	394	$KAl(SO_4)_2$	469
Li_2CO_3	413	$CuCl_2$	318
NaOH	330	$CuSO_4$	370
NaCl	414	$AgNO_3$	413
$NaNO_3$	349	$MgCl_2$	457
Na_2SO_4	445	$MgSO_4$	480
Na_2CO_3	355	$CaCl_2$	400
KOH	296	$SrCl_2$	416
KCl	408	$BaCl_2$	424
KBr	428	$ZnSO_4$	451
KI	388	$CdSO_4$	452
KCN	339	$AlCl_3$	483
KCNS	419	$Al_2(SO_4)_3$	466
KNO_3	346	$SnCl_2$	451
$KClO_3$	397	Pb-acetate	333
K_2SO_4	443	$CrCl_3$	412
K_2CO_3	323	$MnSO_4$	450
$K_2Cr_2O_7$	344	$FeCl_3$	401
$K_4Fe(CN)_6$	336	$CoCl_2$	390
$K_3Fe(CN)_6$	350	$NiCl_2$	420

of the conbustible gas, but suggests that the organic vapour, which was carbonized to produce R_2, plays an impotant rôle in the combustion, as potassium carbonate produced no R_2, while mercuric chloride produced an appreciable amount of it, and, furthermore, the fire-retarding compounds generally produced no or little R_2 and those which yielded a considerable amount of R_2 are not to be fire-resisting compounds as we see in the table. Thus the organic vapour might be considered, so to say, as a kindling material, when cellulose burns[5].

The general process of combustion of cellulose is thought to its preceding thermal decomposition and successive ignition of the combustible materials, such as chars, combustible gases and vapours, and of these materials organic vapour is thought to be the most easily combustible.

Thus the inorganic salts are generally classified according to their effects on the combustion of cellulose as follows:

(I) Those that produce no or little organic vapour by the pyrolysis.

(A) Those that do not lower the ignition temperature of chars appreciably.
$Al_2(SO_4)_3$, $(NH_4)_2SO_4$, $(NH_4)_2HPO_4$, $ZnCl_2$, etc. (fire-resisting compounds)

(B) Those that appreciably lower the ignition temperature of chars.
NaOH, K_2CO_3, $K_2Cr_2O_7$, etc.

(10) Tatibana, *J. Chem. Soc., Japan*, **63**, 924 (1942).
(11) H. Akamatu and H. Hamada, *J. Chem. Soc. Japan*, **66**, 8 (1942).
(12) This sample was made by the Mitsubishi Kasei Co. Ltd.

(II) Those that produce a considerable amount of organic vapour by the pyrolysis.

(A) Those that produce a large quantity of organic vapour.

H_3BO_3, without salt.

(B) Others.

KCl, $HgCl_2$, $BaCl_2$, etc.

The salts in the first group, which produce no or little organic vapour, do not or hardly make cellulose to set flames under normal condition and potassium carbonate, silicate and ferrocyanide, sodium thiosulphate and alminium sulphate and so on belong to this group.

But some salts in the group which lower considerably the ignition temperature of chars, as shown in Table 3, set cellulose on fire without flame, setting the produced chars on fire. Consequently the salts in the first group and those which do not lower the ignition temperature of chars appreciably, such as alminium sulphate, ammonium sulphate and phosphate are to become the fire-retarding salts. And it is to be noted that no or little organic vapour associates to much charcoal yield and thus small quantity of heat evolved at the flames.

In the results of Tatibana[10] alminium sulphate, ammonium sulphate and phosphate have no "ignition temperature," suggesting that the charcoal yielded is not to be set on fire without the aid of the organic vapour, while such salts as potassium carbonate and sodium hydroxide show a lower temperature of ignition probably due to their lowering action of ignition temperature of chars.

In the case of the salts that produce a considerable amount of organic vapours by pyrolysis, cellulose burns in various ways according to the amounts and combustibilities of chars, gases and vapours. But when the organic vapours are so much as in the case of boric acid and untreated cellulose, the kindling material being so much, cellulose is not to be set on fire without flame and thus have no "ignition temperature" as shown by Tachibana[10].

The action of such salts as zinc sulphate, cadmium chloride, ammonium sulphate and phosphate by which cellulose remained as charcoal after the flame had passed over, is to be explained by their comparatively small amount of organic vapour and less lowering action of ignition temperature of chars.

Thus we see that the actions of various inorganic salts are explained from two major factors: the yield of the tarry product and the catalytic action in the combustion of charcoal. Of course, other factors such as the formation of glaze, evolution of inert gas, and absorption of heat by the salts also play a part but only to a minor extent compared with the two major factors.

The chief effect of the fire-resisting compounds upon the above-mentioned carbonization process of cellulose is possibly considered that they promote the polymerization rate by catalysis or ready dehydration from cellulose, consequently, producing little organic vapour.

Summary

(1) The effects of the various inorganic salts on the thermal decomposition of cellulose were investigated.

(2) The combustion of cellulose in the presence of various inorganic salts was measured.

(3) It was suggested that the organic vapour produced by the pyrolysis plays an important rôle in the combustion of cellulose and that the major action of the fire-resisting compounds is to prohibit the yield of this vapour.

(4) The effect of the inorganic salts on the combustion of cellulose were classified and were explained from the two major factors: the yield of organic vapour and the lowering action of ignition temperature of the charcoal.

The author expresses his sincere thanks to Dr. J. Sameshima and Dr. H. Akamatu for their kind guidance and encouragement throughout this work.

Department of Chemistry, Faculty of Science the University of Tokyo, Tokyo

Studies on Dielectric Behavior of Bound Water in Timber in the High Frequency Region

By Masatami TAKEDA

(Received March 5, 1951)

Introduction

It has been well-known up to this time that the dielectric properties of timber remarkably depend upon the water contained. Recently, a new industry of utilizing the high frequency electric waves as a heat source for drying timbers or for gluing wood pieces together was developed in this country,[1] and many factors involved in the process were examined, *e. g.*, the amount of water contained, the temperature of the treatment and the wave-length of electric wave to be employed. Indeed, it is often regarded important as well as interesting to investigate why the water contained in timber has such a predominant effect upon its dielectric properties.

In the present paper, the author has intended to report the dielectric behavior of timber in the high frequency region and its possible interpretation of the results. Special attentions were paid to the measurements of the microwave region, where remarkable dielectric dispersion and absorption are expected to occur. And in comparing the dielectric behavior of pure water and that of bound water in timber, we hoped to obtain some useful informations about the state of the latter.

Experimental Method

The measurements of complex dielectric constants were carried out

1) at 3×10^3 M. C. by the free wave method[2,3]
2) *ditto* by the wave guide method[4,5]
3) at 300 M. C. by the impedance bridge method[6]
4) in the region of 0.2—15 M. C. by the dynatron method[7]
5) d. c. conductivity by the usual galvanometer method.

The timbers of the species *tilia* (product in Hokkaido) were chosen as the experimental materials. The wood pieces to be tested were prepared in three different ways, *i. e.*, (a) cut perpendicular to the wood vessels, (b) to the medullary rays and (c) parallel to the both. The samples which were dried for several hours in a drought at the temperature of 100° were assumed as the standard material for zero-water-content. They were dried in a bath and then put into a vessel, the humidity of which was kept constant by the use of H_2SO_4 solution. The amount of absorbed water was determined with a chemical balance.

Experimental Results

The measurements of dielectric constant and loss factor were made in the region of 0.2-3000 M. C. for the samples of various water-contents (from 0 to 14% at 300 and 3000 M. C.; from 0 to 20% in the region of 0.2—15 M. C.). The results were shown in Figs. 1-6, where ε' denotes dielectric constant, ε'' loss factor, σ

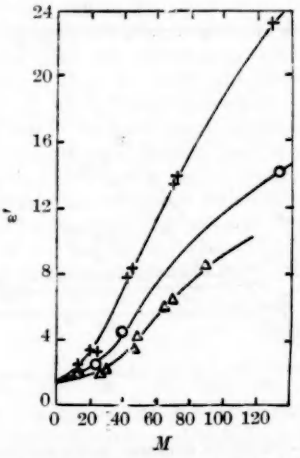

Fig. 1.—Dielectric constant at 3000 M. C. (room temp.): ×, the electric field ∥ wood vessels; ○, the electric field ∥ medullary rays; △, the electric field ⊥ wood vessels and ⊥ rays.

(1) "Theory and Application of High Frequency Phenomena," ed. by Asami (1950). Research Institute of Applied Electricity, Hokkaido University.
(2) Yasumi, This Bulletin, **24**, 53 (1951).
(3) This measurement was made with the help of Mr. K. Nukazawa, Research Institute of Applied Electricity, Hokkaido University.
(4) Matsumoto and Suzuki, *Bull. Technology* (Hokkaido University) **1**, 138 (1949).
(5) This measurement was carried out in the collaboration with Prof. Suzuki of the Department of Electric Engineering, Faculty of Technology, *ditto*.
(6) Morita, *J. Inst. Elec. Eng.* (Japan)., **65**, 59 (1946).
(7) Nishi and Sakamoto, *ibid.*, **59**, 699 (1940).

conductivity, f frequency, ω angular frequency and M water-content (in weight percentage), respectively.

In Figs. 1 and 2, dielectric constants and loss-factors measured at 3000 M. C. are plotted against the moisture-content, while in Fig. 3 the results obtained at 300 M. C. are shown. In all these diagrams the variations in ε' and ε'' due to the inhomogeneity of the material are clearly observed.

In Figs. 4 and 5 are shown the results obtained for a wide range of frequencies——in Fig. 5 the direct current measurement is also included. In Fig. 4 the increase in ε' with the increase of water-content is found to decrease with the increase in frequency. It is further to be noted that these increases in value of ε' are not marked in the range of 0 to 5 %. Moreover, it is interesting that the curves

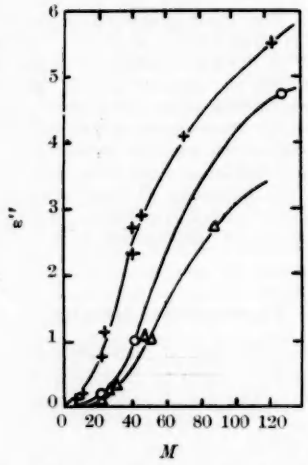

Fig. 2.—Loss factor at 3000 M. C. (room temp.) ×, ○, △, *ditto.*

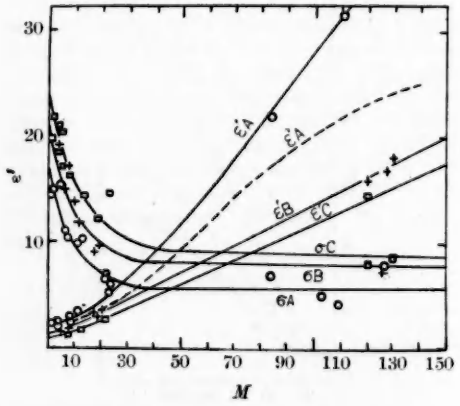

Fig. 3.—Dielectric constant and conductivity at 300 M. C. (full line) and at 3000 M.C. (broken line) (temp. 15°±2°C.): A, the electric field ∥ the wood vessels; B, the electric field ∥ the medullary rays; C, the electric field ⊥ vessels and rays.

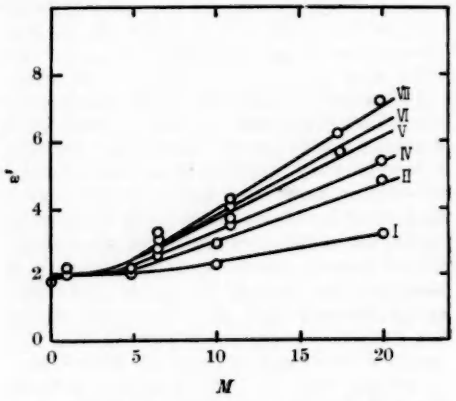

Fig. 4.—Dielectric constant and water-content (15°C.): I, 3×10^9 cycles; II, 3×10^8 cycles; IV, 1.0×10^7 cycles; V, 3×10^6 cycles; VI, 1×10^6 cycles; VII, 0.4×10^6 cycles.

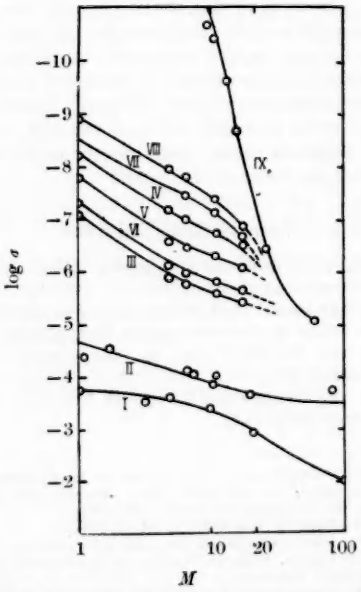

Fig. 5.—Conductivity and water-content (15°C.): I, 3×10^9 cycles; II, 3×10^8 cycles; III, 15×10^6 cycles; IV, 10×10^6 cycles; V, 3×10^6 cycles; VI, 1×10^6 cycles; VII, 4×10^5 cycles; VIII, 2×10^5 cycles; IX, d. c.

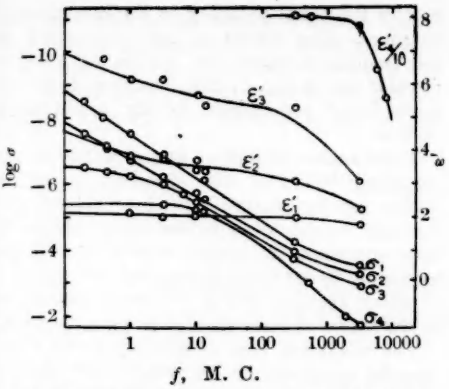

Fig. 6.—Dielectric constant and conductivity (15°C.).

ε'_1, σ_1	water-content	3.5%
ε'_2, σ_2	"	10%
ε'_3, σ_3	"	20%
ε'_4, σ_4	pure water	

of $\log \sigma$ *versus* M in Fig. 5 are similar to those of the dried carrot obtained by Dunlap and Makover[8].

The values of ε' and $\log \sigma$ of the samples of the same water-content are plotted against the frequency in Fig. 6. The dielectric constants of the samples of the 10 % and 20 % water-contents decrease with the increase in frequency, while $\log \sigma$ generally increases with the increase of frequency. On closer examination, it appears that the inflection points of the curves for low-water-content shift to the side of lower frequency than those for high-water-content and that for pure water.

Discussion

To begin with the discussion, we must admit that our material of study, timber, is a very complicated substance to which no heterogeneous theory of dielectrics is quite applicable. Therefore we will not venture to give any complete explanation for the results observed but rather wish to present some useful notes connected with this topic. First of all, we will consider the dielectric behavior of pure water. (See the curves of ε'_4 and σ_4 in Fig. 6.) The relation between dielectric constant (or loss factor) and the frequency was treated theoretically by Debye[9] on the basis of dipole rotation. If we assume the Onsager's inner field instead of the Clausius-Mosotti's relation which was adopted in the Debye's original theory, the dielectric quantities will be expressed as follows:

$$\left.\begin{aligned} \varepsilon' - i\varepsilon'' &= \varepsilon_{(\infty)} + \frac{\varepsilon_0 - \varepsilon_{(\infty)}}{1 + i\omega\tau} \\ \text{and} \qquad \sigma &= \frac{\omega\varepsilon''}{4\pi} \end{aligned}\right\} \quad (1)$$

where $\varepsilon_{(0)}$ and $\varepsilon_{(\infty)}$ are dielectric constants at $\omega = 0$, and $\omega = \infty$ respectively, τ is the relaxation time which differs from that of Debye by a constant factor.

We put the values $\varepsilon_{(0)} = 81$, $\varepsilon_{(\infty)} = 1.8$ and $\tau = 9.4 \times 10^{-12}$ sec^{-1} (at 15°) into Eq. (1), and the calculated results are found to be in good accord with the experimental data for angular frequencies ω above 50 M. C.

As often pointed out, the following equation holds in the low frequency range.

$$\log \sigma = 2 \log f + \text{const.} \qquad (2)$$

If the relation that $\omega < \frac{1}{\tau}$ is assumed, then Eq. (2) can easily be derived from Eq. (1). If water has an appreciable d. c. conductivity, σ_{ion} which arises from the movement of ions, σ is expressed as follows:

$$\sigma = \frac{(\varepsilon_{(0)} - \varepsilon_{(\infty)})}{4\pi} \cdot \frac{\omega^2\tau}{1 + \omega^2\tau^2} + \sigma_{\text{ion}} \qquad (3)$$

(σ and σ_{ion} in e. s. u.)

The experimental values of σ in the region of frequencies less than 50 M. C. are found to agree with that of Eq. (3).

The dielectric constant of timber in general increases with the increase in water-content. Further, it is to be noted that the dispersion region of the dielectric constant of timber (10 %—20 % water-content) shifts to the side of the longer wave length than that of pure water[10]. This fact is an indication that the relaxation time of bound water in timber has a larger value than that of pure water. According to Debye, the relaxation time τ is related to internal viscosity η by the following equation.

$$\tau = \frac{4\pi\eta a^3}{kT} \qquad (4)$$

where a is the radius of rotating molecule. If the internal viscosity η of bound water happens

(8) Dunlap and Makover, *J. Phys. Chem.*, **49**, 601 (1945).
(9) Debye, "Polare Molekeln," Leipzig, 1929, s. 108.
(10) The dielectric behavior of ethyl alcohol absorbed by silica gel was studied by Higuti and it was found that dielectric dispersion shifted to a longer wave length than that of pure ethyl alcohol. This is in complete agreement with our observation.

to be larger than that of pure water[11,12], it will be natural to conclude that its relaxation time will exceed that of free water.

The experimental results for the wet timbers cannot, of course, be treated by Eq. (1). Trying to find a more general relation than that of Debye, Cole and Cole[13] succeeded in proposing the following empirical relationship,

$$\varepsilon' - i\varepsilon'' = \varepsilon_{(0)} + \frac{\varepsilon_{(0)} - \varepsilon_{(\infty)}}{1 + (i\omega\tau)^{1-\alpha}} \qquad (5)$$

where τ is a most probable relaxation time and α is an empirical constant having a value between 0 and 1. The data for timbers are plotted in Fig. 7, as required by the relation of Cole and Cole (see Table 1).

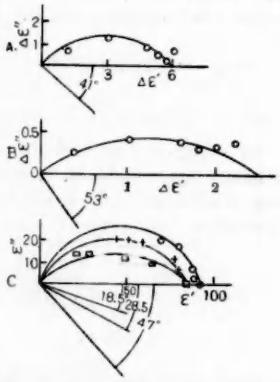

Fig. 7.—The Cole-Cole diagram.
Timber of A, 20%; B, 10% water-content. C, cane sugar solutions: ○, 30%; ×, 50%; □, 65%.

Table 1

Water-content in the sample, %	τ, $\times 10^{-10}$ sec.	α
10	1.9	0.59
20	1.3	0.45

For the comparison's sake, the values for sucrose solution[14] are also plotted in Fig. 7. The relation between the concentration and values of α in sucrose solution is similar to that of the water-content and α in the case of timber. Therefore, it may be concluded that the dielectric behaviors of wet timbers are represented by the two parameters, α and τ, with the equal accuracy to the case of sugar solutions. The values of $\Delta\varepsilon''$ measured at low frequency region do not lie on a semi-circular arc in Fig. 7, this departure from the curve being attributable to the conductivity of ion.

From earlier studies of bound water, it was suggested[15,16] that the absorbed water in timber can be grouped into three classes. (1) Strongly bound water in the region of 0—5% water-contents, (2) weakly bound water in the region of 5—30% water-contents — so-called capillary absorbed water, (3) nearly free water in the region of more than 30% water-content.

The relaxation time of strongly bound water may be considered to be very large that the dielectric constant should have a small value — this being revealed by Figs. 1, 3 and 4. The fact that the rate of increase in ε becomes constant in the range of the greater water-content, *i. e.*, more than 30%, suggests that the water of this range is nearly free in the timber.

Lastly we may add that Nukazawa and Takeda[17] have examined also some of our microwave data by the use of the theories due to Maxwell, Wagner[18], Sillars[19] and Ozawa[1,20] for the heterogeneous dielectrics. The results appeared to be in good accord with the assumption of bound water, since we found always remarkably large loss factor and smaller dielectric constant for component water at 3000 M. C.

Summary

1. Dielectric constants and loss factors of timber *tilia* containing various amounts of water have been measured in the region of frequencies of 0.2—3000 M. C.

2. The dielectric properties of these materials at the high frequency region are found to depend upon the rotation of dipoles of water, free and bound, in timber. The empirical relation proposed by Cole and Cole are utilized for the explanation.

3. Their dielectric properties at lower frequencies may be attributed to the other causes such as the movement of ions in the material.

The present research was undertaken when the author was a member of Research Institute of Applied Electricity, Hokkaido University

(11) Higasi, *Kagaku* (*Science*) **17**, 82, 83, 126, (1947).
(12) Higasi and Nukazawa, *Kagakuno-Kenkyu* (*Chemical Researches*) **1**, 28, (1948).
(13) Cole and Cole, *J. Chem. Phys.*, **6**, 385 (1938).
(14) Slevogt, *Ann. Phys.*, (5) **36**, 141 (1936).
(15) Stamm, *Ind. Eng. Chem.*, **21**, 94 (1929).
(16) Stamm, *J. Phys. Chem.*, **39**, 121 (1934).
(17) Nukazawa and Takeda, *Kagaku* (*Science*), **17**, 181 (1947).
(18) Wagner, *Elektrotech.*, **2**, 371 (1914).
(19) Sillars, *J. Inst. Elec. Eng.*, **80**, 378 (1937).
(20) Asami, Higasi and Ozawa, *Nature*, **165**, 195 (1950).

and he wishes to express his sincere thanks to Professor K. Higasi for his kind guidance. His thanks are also due to Mr. Nukazawa and Mr. Suzuki for their kind cooperation, and Dr. Yasumi for his help in translating the original manuscript into English, and the Ministry of Education for the donation of the Grant in Aid for Scientific Research.

Tokyo College of Science, Sinjuku, Tokyo

Magnetic Property and Resonance Character of Cyclooctatetraene (C_8H_8)

By Shoji SHIDA and Saburo FUJII

(Received April 25, 1951)

Introduction

If cyclooctatetraene (C. O. T.) is assumed to have a regular eight-membered ring structure, it may be paramagnetic in the ground state. This has been theoretically suggested by E. Hückel[1] in his earlier quantum mechanical treatment and shown recently also by Y. Mori, I. Tanaka and S. Shida[2] from the standpoint of the antisymmetrical molecular orbital theory including electron repulsions.

On the other hand, if it is not paramagnetic but diamagnetic on account of some reasons, it will have more or less diamagnetic anisotropy due to resonance in analogy with benzene and other aromatic molecules.

In the course of the study the following fact has come to be clear that R. C. Pink[3] and W. Klemm[4] had obtained -51.9×10^{-6} and -55.6×10^{-6} respectively as the molecular diamagnetic susceptibility of C. O. T. The difference between the above two values, which is beyond the usual experimental errors in susceptibility measurements, may be considered to be dependent upon impurities in the C. O. T. used by them, and their interpretations for the magnetic property seem to be different from ours so far as we can know from the available abstracts[5] of their works.

Therefore it is worthwhile to report our new susceptibility measurements for purified C. O. T. and to describe our opinions for this magnetic property, especially for the relationship between the diamagnetic anisotropy and the resonance character, on the basis of its probable structures[6]~[11], its thermal data[12]~[14] and the quantum mechanical calculations[2],[15] on its electronic levels.

Experimental

Our apparatus for magnetic susceptibility measurements is a Weiss-Fõex type[16] with several refinements and the main part is shown diagramatically in Fig. 1.

This main part is doubly covered with glass plates to prevent it from air disturbance. Passing a constant direct current of 20 amperes through this magnet, the field strength between the pole-pieces, 17 mm. apart from each other, is about 10,000 gausses. According to the tests with several common substances this apparatus is proved to be useful with an error of 0.5 percent for determinations of mass susceptibilities of 10^{-6} order and able to detect its temperature dependence exceeding 0.5 percent over the temperature range 20° to 100°C.

(1) E. Hückel, *Z. Physik*, **70**, 204 (1931); *J. de phys. et rad.*, **6**, 347 (1935).
(2) Y. Mori, I. Tanaka and S. Shida, This Bulletin, **23**, 168 (1950).
(3) R. C. Pink and A. R. Ubbelohde, (a) *Nature*, **160**, 502 (1947); (b) *Trans. Faraday Soc.*, **44**, 708 (1948); (c) *Chemical Abstracts*, **43**, 2479f (1949); (d) *ibid.*, **44**, 6212f (1950).
(4) W. Reppe, "Acetylene Chemistry," 1946.
(5) References 3a, 3c, 3d, and 4.
(6) O. Bastiansen, O. Hassel and A. Langseth, *Nature*, **160**, 128 (1947).
(7) O. Bastiansen and O. Hassel, *Acta Chemica Scandinavica*, **3**, 209 (1949).
(8) E. P. Lippincott, R. C. Lord and R. S. MacDonald, *J. Chem. Phys.*, **16**, 548 (1948).
(9) H. S. Kaufman, I. Fankuchen and H. Mark, *J. Chem. Phys.*, **15**, 414 (1947).
(10) H. S. Kaufman, I. Fankuchen and H. Mark, *Nature*, **161**, 165 (1948).
(11) R. Hedberg and V. Schomaker, Annual Meeting of Am. Chem. Soc., 1949.
(12) E. T. Prosen, W. H. Johnson and F. D. Rossini, *J. Am. Chem. Soc.*, **69**, 2068 (1947).
(13) E. T. Prosen, W. H. Johnson and F. D. Rossini, *ibid.*, **72**, 626 (1950).
(14) D. W. Scott, M. E. Gross, G. D. Oliver and H. M. Huffmann, *J. Am. Chem. Soc.*, **71**, 1634 (1949).
(15) I. Tanaka and S. Shida, This Bulletin, **23**, 54(1950).
(16) G. Foex and R. Forrer, *J. phys.*, **7**, 180 (1926).

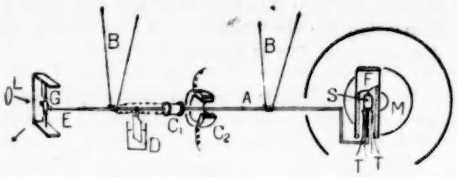

Fig. 1—Weiss-Fõex Balance: A, quartz rod; B, fine copper wire; C_1, the 1-st coil; C_2, the 2-nd coil; D, oil damper; E, magnetized needle; F, electric furnace; G, mirror suspended by fine bronz ribbon (its back is pasted with polished thin steel plate); L, lens; M, magnet; S, sample vessel; T, thermocouple.

The C. O. T. used in the present measurement was obtained through the courtesy of Professor S. Murahashi and Dr. N. Hagiwara[17], who prepared it with the catalytic polymerization of acetylene in autoclave and purified it by means of several fractional distillations under a low pressure of nitrogen. This substance is a transparent yellow liquid (m. p. −7.5°, b. p. 95.6° at 185 mm. Hg) and stored in an evacuated tube in the dark because it becomes turbid brown in a day if opened in air. Before each measurement this substance, not including any detectable amount of styrene, was distilled several times *in vacuo* and the last middle portion always used.

Our measured value of the mass susceptibility of this C. O. T. at 30° is

$$(-0.518\pm0.003)\times10^{-6}$$

hence the molecular susceptibility

$$(-53.9\pm0.3)\times10^{-6}$$

This value is between those obtained by W. Klemm and by R. C. Pink. In the measurement of the temperature dependence of susceptibility for this substance the experiment was carried out with the sample distilled in an evacuated small glass vessel for susceptibility measurement and the correction for the vessel was done under the condition of it being evacuated. The magnitude of force acting on the sample liquid in a non-homogeneous magnetic field depends sharply upon the volume and the position which are occupied by the sample between both pole-pieces. Therefore the magnitudes of force acting on the constant mass at various temperatures are, though slightly, detectably different from each other owing to the volume change with temperature of the sample liquid. The fact indicates that the relation between the magnetic force and the volume of sample is necessary to be determined in this experiment. The correction[18] for the effect described above was also taken into account in the present measurement.

According to these three measurements the temperature dependence of the mass susceptibility of C. O. T. could not be detected over the temperature range 30° to 80°C. with an experimental error of 0.5 percent.

Discussion

Though we cannot determine the reliable order for the three different values of the mass susceptibility of C. O. T. because the detailed reports on W. Klemm's and R. C. Pink's experiments cannot be obtained, this substance is now clearly proved to have a temperature independent diamagnetism and therefore the possibility of a spin paramagnetism, as suggested by E. Hückel, excluded. Our purpose for the measurement of the temperature dependence of this diamagnetism was to examine the possibility of a small energy difference between the diamagnetic ground state and the lowest triplet one as well as that of a mixture of diamagnetic and spin paramagnetic isomers, this latter one being assumed in the first report[3a] by R. C. Pink and A. R. Ubbelohde. But our result does not support these possibilities.

Next it is important to consider the diamagnetic anisotropy of this molecule in comparison with aromatic and hetero-cyclic ones composed of conjugated double bonds, for the previous authors[3),4)] did not pay any attention to this property. The diamagnetic anisotropy of ring-shaped molecules composed of conjugated double bonds is generally recognized to be induced by the free migration of resonating $p\pi$ electrons along the molecular network under an external magnetic field, and therefore it can be represented qualitatively with circulating electric currents along the molecular network. The molecular structure of C. O. T. has not yet been determined definitely, but the most probable one may be D_{2d}[9)~11)], while D_{4d}[6),7)] and D_4[8)] are also recently reported by different authors.

Then, with these structures and the models shown in Fig. 2, the anisotropic parts to x and y directions may be nearly negligible because each component of the diamagnetic currents is canceled out vectorically by oneself from the above view-point.

According to this consideration the molecular susceptibilities to the both directions have to be equally 4/3 times of that of benzene, *i. e.*, about -49.7×10^{-6}. Then, from the experimental mean molecular susceptibility -53.9×10^{-6} and the values to x and y directions, the

(17) The members of the Institute of Scientific and Industrial Research, University of Osaka.

(18) This correction was obtained by the use of toluene. The mass susceptibility of toluene has not a temperature dependence exceeding 0.5 percent over the temp. range 10° to 50°. (G. F. Boeker, *Phys. Rev.*, **43**, 756 (1933)).

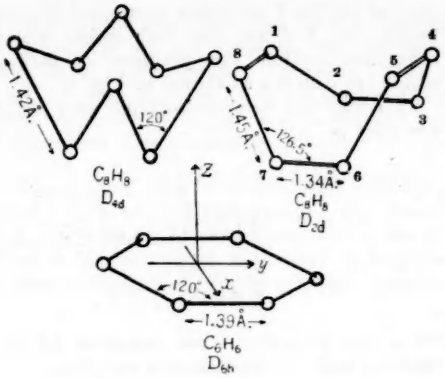

Fig. 2.

anisotropic part[19] to z-direction is estimated as about -12.6×10^{-6} per mole, that is, about 23 percent of that of benzene. This estimated anisotropy is very small in spite of the fact that this molecule has eight pπ electrons and larger projected area on the xy plane than that of benzene.

On the other hand, the estimated resonance energy of this compound is also small and about 2.9 kcal. per mole, it being about 7 percent of that of benzene. It is calculated from the following thermal data determined recently;

$$8C(\text{graphite})+4H_2(\text{gas})=C_8H_8(\text{liquid})+(60.82\pm0.32)\ \text{kcal./mole}^{[13]},$$

the heat of vaporization of liquid C_8H_8 is 10.300 $\pm$0.075 kcal./mole[14] and the bond energies[20]

$$\begin{cases}C-C\ \ldots.\ 60.3\ \text{kcal. per mole}\\ C=C\ \ldots.102.9\ \text{„ „ „}\\ C-H\ldots.\ 87.15\ \text{„ „ „ .}\end{cases}$$

R. C. Pink and A. R. Ubbelohde[3a] have obtained 25.4 kcal./mole for this resonance energy. The old value used by them for the heat of formation of this compound is considered to have some uncertainty and therefore their question that C. O. T. is magnetochemically aliphatic rather than aromatic in spite of its considerable resonance energy may not be fit. From these relationships between resonance energies and diamagnetic anisotropies of C. O. T. as well as aromatic and hetrocyclic molecules composed of conjugated double bonds we can understand that the larger anisotropy a molecule has, the more remarkable its resonance character is. This phenomenon can be explained qualitatively from the quantum mechanical view-point by the fact that these two properties are both directly related to the resonance integrals of pπ electrons.

According to the atomic and molecular orbital calculations[2),(15)] on the electronic levels of this molecule the exchange or resonance integrals between any adjacent carbon atoms in the case of D_{4d} and these between the 1-st and 2-nd carbon atoms in D_{2d} in Fig. 2 are smaller than those of benzene. Also the calculated resonance energy[2] in the case of D_{2d} on the basis of the L-C-A-O approximation is 2.7 kcal./mole, it being consistent with the value estimated from thermochemical data.

Therefore the small anisotropy of this molecule can be also explained by the fact that the small resonance integral means the difficulty of free migration of pπ electrons along the molecular network under an external magnetic field. Then it is interesting to discuss this anisotropic part on the basis of Langevin's classical theory[21] and the molecular orbital method by F. London.[22] The latter obtained an excellent agreement with experiments in the calculation of the anisotropies of aromatic molecules. According to P. Langevin the anisotropic part of a simple ring-shaped molecule with n migrating pπ electrons can be written

$$\Delta\chi_M=-\frac{Ne^2}{4\pi mc^2}\sum^{n}\overline{r_i}^2 \quad \ldots\ldots\ldots(1)$$

where N is the Avogadro number and $\overline{r_i}^2$ mean square radius of the i-th migrating pπ electron along the molecular ring.

In the cases of benzene, pyridine, furane, pyrole, thiophene and cyclopentadiene, all of which have plane structures and relatively large resonance energies, the calculated anisotropies[23] from Eq. (1) are in agreement with the values estimated from the Pascal additivity law within the maximum error of about 10 percent. However, the calculated values for C. O. T. as D_{4d} and D_{2d} are -103.7×10^{-6} and -155.6×10^{-6} respectively, and obviously they are quite different from the value estimated by us, *i. e.*, -12.6×10^{-6}. Hence Langevin's theory may be applied only to the molecule with a plane structure and a remarkable resonance character.

(19) G. Hazato, *J. Chem. Soc. Japan*, **64**, 483 (1943).
(20) J. T. Cotrell and L. E. Sutton, *J. Chem. Phys.*, **15**, 685 (1947).
(21) E. C. Stoner, "Magnetism and Matter," Methuen & Co. Ltd, London, 1934, p. 107.
(22) F. London, *J. de phys. et rad.*, **8**, 397 (1937).
(23) G. Hazato, *J. Chem. Soc. Japan*, **64**, 622 (1943).

Now we shall apply the London theory to this molecule to see what results we can get from this method. If the field perturbation is neglected, his theory is reduced to a simple type of the one-electron approximation, and then the ground electronic states calculated in this case are illustrated in Fig. 3.

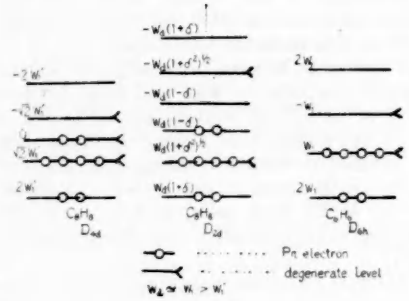

Fig. 3.

In Fig. 3 it is shown that both D_{2d} and D_4 structures are diamagnetic but D_{4d} should have a spin paramagnetism owing to a degenerate level occupied by only two electrons and so the calculation of the anisotropic part for D_{4d} may be meaningless. Therefore we shall calculate the anisotropy in the case of D_{2d}, and the present calculation follows, for the convenience' sake, the same notation and procedure as London's paper.

If $\left(\frac{x_k+x_l}{2} \pm \xi_{kl}, \frac{y_k+y_l}{2} \pm \eta_{kl}\right)$ are two xy-coordinates where the overlap between Pz wave functions in the k-th and the l-th carbon atoms is maximum, and we put

$$\theta_{kl} = \frac{\pi e}{hc}[(x_k-x_l)\eta_{kl}-(y_k-y_l)\xi_{kl}],$$

then the anisotropic part due to a $p\pi$ electron in the p-th energy state is expressed as follows:

$$\chi_p = -|W_a| \times \left\{ \frac{(\theta_a^2+\delta^2\theta_s^2)+\left(\frac{\pi^2e^2S^2}{16h^2c^2}+\theta_a^2+\theta_s^2\right)\delta\cos\frac{2\pi}{4}p}{\left(1+2\delta\cos\frac{2\pi}{4}p+\delta^2\right)^{1/2}} + \frac{\left(\frac{\pi^2e^2S^2}{16h^2c^2}+\theta_a^2+\theta_s^2\right)\delta^2\sin^2\frac{2\pi}{4}p}{4\left(1+2\delta\cos\frac{2\pi}{4}p+\delta^2\right)^{3/2}} \right\}, \quad \ldots(2)$$

where $\theta_a=\theta_{81}$, $\theta_s=\theta_{12}$, $\delta=W_s/W_a<1$. S is the projected molecular area on the xy-plane and W_s, W_a are the resonance integral between the 1-st and the 2-nd carbon atoms and the one between the 1-st and the 8-th carbon atoms respectively. Here the positions of carbon atoms are denoted as shown in Fig. 2.

Therefore the total anisotropic part to z-direction is

$$\Delta\chi_M = 2(\chi_{-1}+\chi_0+\chi_1+\chi_2) = -4|W_a|\left[\delta^2\left(\frac{\pi eS}{2hc}\right)^2\left\{\frac{1}{(1+\delta^2)^{3/2}}-\frac{1}{1-\delta^2}\right\} +\theta_a^2+\frac{\theta_a^2+\delta^2\theta_s^2}{(1+\delta^2)^{1/2}}\right]. \quad \ldots\ldots\ldots(3)$$

Using the numerical data measured by K. Hedberg and V. Shomaker[11] we obtain $S=7.9(\text{Å}^2)$, $|\theta_a|=0.32\left(\frac{2\pi e}{hc}\right)(\text{Å}^2)$ and $\theta_s \doteqdot 0$. Then assuming $\delta=0.4$[2] we obtain

$$\Delta\chi_{C_8H_8,D_{2d}} = +0.26|W_a|\left(\frac{2\pi e}{hc}\right)^2, \quad \ldots(4)$$

while for benzene

$$\Delta\chi_{C_6H_6,D_{6h}} = -5.75|W_1|\left(\frac{2\pi e}{hc}\right)^2, \quad W_1 \simeq W_a.$$

Eq. (4) indicates the anisotropic part for D_{2d} being weak paramagnetic and furthermore Eq. (3) represents that the anisotropy becomes more paramagnetic as δ approches to 1 over 0.4.

These results are obviously in contradiction with experiments and physical aspects. The calculated results in the case of D_4 are identical with that of D_{2d}, though the numerical values of W_a, δ, S, δ_a and θ_s are different from those in D_{2d}. Considering the above discussions both of Langevin's theory and London's method in the original form cannot explain the small diamagnetic anisotropy of C. O. T. quantitatively or even qualitatively. The question why the London's method cannot apply to this molecule with his original procedure is remained unsolved and under investigation.

Summary

We have obtained -53.9×10^{-6} at 30° as the molecular diamagnetic susceptibility of purified cycloöctatetraene, and its temperature dependence exceeding 0.5 percent over the temperature range 30° to 80° has not been detected. The diamagnetic anisotropy of this molecule has been estimated -12.6×10^{-6} per mole on some assumptions, and the resonance energy 2.9 kcal. per mole from the thermal data.

The relationship between the small anisotropy and the weak resonance character of this

molecule has been discussed and explained qualitatively on the basis of the quantum mechanical considerations. Langevin's theory and the original procedure of London's method have been found to be unsuitable for the explanation of this small anisotropy.

The authors wish to express their appreciation to Professor M. Tamura at the Kyoto University for his encouragement and to Mr. I. Tanaka for his helpful discussion during the course of this work. They are also grateful to Professor O. Murahashi and Dr. N. Hagiwara at the Institute of Scientific and Industrial Research, University of Osaka, for their kind offer of cycloöctatetraene and for their helpful advice. The cost of this research was defrayed from the Scientific Research Encouragement Grant from the Ministry of Education, to which the authors' thanks are due.

Laboratory of Physical Chemistry,
Tokyo Institute of Technology, Tokyo

On the Action of Carriers in the Catalytic Hydrogenation of Acetylene by Palladium Catalyst

By Kenzi TAMARU

(Received April 28, 1951)

Introduction

The author previously investigated[1] the hydrogenation of acetylene on Pd-alumina (1:100) catalyst by the static method. It was found that the hydrogenation of acetylene proceeds in two distinct steps at room temperature. The first step consists of the reduction and polymerization of acetylene, and the second step the hydrogenation of ethylene to ethane. The second step started after all acetylene was used up, accompanying a sudden increase in the rate of hydrogenation, and this phenomenon was explained by the strong adsorption of acetylene on the surface of the catalyst. Poisoning or retarding both steps of the hydrogenation simultaneously, it was suggested[2] from the kinetical treatment of the reaction that the hydrogenation of acetylene occurs on the various "active regions" with different proportions from that of ethylene.

Palladium catalysts which was deposited on kieselguhr with various dispersities proceeded the hydrogenations of the two hydrocarbons with different relative rates. Hence, this fact was considered to suggest[3] the difference of the dispersity of the catalyst to have connection with the appearance of the various "active regions" of the catalyst surface with different ratios.

In this study experiments were carried out on the palladium catalyst deposited on the various carriers and the rôle of the carrier, along with the mechanism of the hydrogenation of acetylene, was considered.

Experimental

Palladium was deposited on the various carriers by the similar method with that of the previous experiments, that is, suspending the carriers in the palladium chloride solution, potassium hydroxide solution and formaldehyde were added to deposit the palladium on the carriers. Silica gel, french chalk, carbon black, active charcoal, quartz sand, Japanese acid clay, alumina and kieselguhr were used as carriers[4] and the ratio of palladium to the carrier was 1/100 for each carrier.

The experiments were carried out by the static method and their procedure was the same as the previous experiment[1]. The results of the several experiments at 30.0° are shown in Fig. 1. The

(1) Kenzi Tamaru, This Bulletin, **23**, 64 (1950).
(2) Kenzi Tamaru, This Bulletin, **23**, 180 (1950).
(3) Kenzi Tamaru, This Bulletin, **23**, 184 (1950).

(4) The used carriers were as follows: Silica gel and Japanese acid clay were prepared by the Takeda Pure Chemicals Ltd. Osaka; French chalk by the Hirasawa Pharmaceutical Laboratory, Tokio; carbon black by the Nihon Kasei Co. Ltd.; active carbon (powder) by E. Merck, Darmstadt, and quartz sand by the Schering-Kahlbaum A. G. Berlin.
The granular active carbon was prepared from the charcoal impregnated by phosphoric acid and each granule was about 0.02 to 0.05 g. in weight.

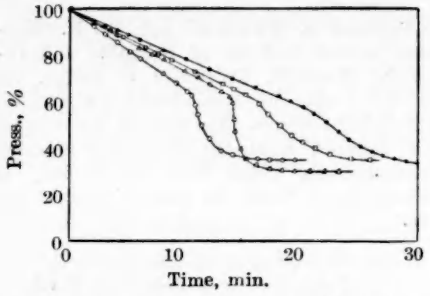

Fig. 1.—Hydrogenation of acetylene by Pd-catalyst on the various carriers at 30°.

	Total press., mm. Hg	C_2H_2, %
—□——□—: Pd-French chalk (0.210 g.)	439	32.5
—●——●—: Pd-Japanese acid clay (0.165g.)	474	36.1
—△——△—: Pd-active carbon (Merck) (0.519 g.)	402	33.7
—○——○—: Pd-carbon Black (0.545 g.)	422	35.0

change of the composition of the reactant with time was qualitatively similar with that in the experiments on Pd-alumina or Pd-kieselguhr catalyst in the preceding papers, and the hydrogenation of acetylene first proceeded linearly with time, and when acetylene was used up, the second step, or ethane formation, began with a faster rate.

When the granular active carbon was used as a carrier, the change of the total pressure of the reactant with time was very different from Fig. 1, as shown in Fig. 2 by the full line, and the

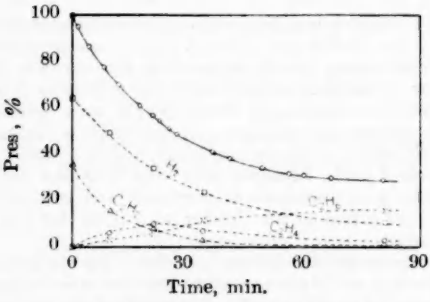

Fig. 2.—Hydrogenation of acetylene by Pd-granular active carbon at 30°: Catalyst, 0.425 g.; total press., 511 mm.-Hg; C_2H_2, 36.0%.

reaction rate was appreciably different according to the sizes of the granules. The change of the composition of the reactant was given by the broken lines in the figure. In this case no inhibition of the ethane formation by acetylene was observed and both hydrogenations of acetylene and ethylene were simultaneously occurred, showing a typical successive reaction.

But when the catalyst was powdered in the mortar, the hydrogenation proceeded in a different way from the granular one, as shown in Fig. 3 by the full and the broken lines, that is, a new reflection point appeared, which is indicated by the arrows in the figure. The change of the composition of the reactant was shown by the dotted lines in Fig. 3 in the case of the initial

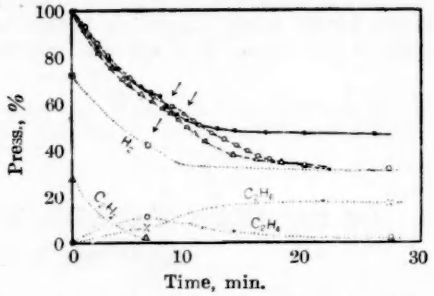

Fig. 3.—Hydrogenation of acetylene by Pd-powdered active carbon and Pd-silica gel at 30°.

	Total press., mm.-Hg	C_2H_2, %
--○----○--: Pd-powdered active carbon (0.248 g.)	495	36.7
—●——●—: Pd-powdered active carbon (0.096 g.)	514	27.6
—·△—·—·△—·: Pd-silica gel (0.620 g.)	405	36.4

composition of 27.6% acetylene content. The ethane formation was already observed while acetylene was being hydrogenated and the reflection point corresponded to the moment that all acetylene was consumed.

The result of the Pd-silica gel catalyst is shown in Fig. 3 by the chain line and this is very similar to that of Pd-powdered active carbon catalyst. It was shown by gas analysis that the reflection point was the point that all acetylene was used up and that ethane formation was to be seen before the point, similarly with the case of Pd-powdered active carbon catalyst.

When quartz sand was used as a carrier the result was appreciably different from the other carriers, and ethane and ethylene formations proceeded simultaneously as shown in Fig. 4. When the initial composition was changed, the reaction proceeded, for example, as shown in Fig. 5 and no self-retardation of acetylene was observed in this case.

The hydrogenation rate of acetylene and ethylene by palladium on the various carriers were shown in Table 1, where the reduction rate of ethylene to ethane was obtained through the hydrogenation of ethylene without retardation of polymers and was given in the table by the reaction constant of the first order reaction.

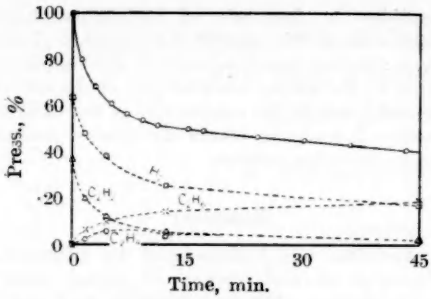

Fig. 4.—Hydrogenation of acetylene by Pd-quartz sand catalyst at 30°: Catalyst, 0.387 g.; total press., 521 mm.-Hg.; C_2H_2, 36.5%.

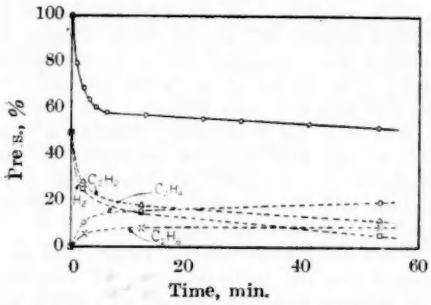

Fig. 5.—Hydrogenation of acetylene by Pd-quartz sand catalyst at 30°: Catalyst, 0.467 g.; total press., 550 mm.-Hg; C_2H_2, 49.8%.

Table 1

The Hydrogenation Rates of Acetylene (V_1) and Ethylene (k_2) by Palladium on the Various Carriers

Carriers	V_1*, %/10 min.	k_2
Alumina	21.0	20.0
Kieselguhr	25.0	24.6
Japanese acid clay	13.3	—
French chalk	11.9	8.0
Carbon black	6.6	6.0
Active carbon (Merck)	5.2	9.0
Powdered active carbon	28.1	—
Silica gel	11.8	—
Quartz sand	59.5	—

* The initial rate of hydrogenation of acetylene per gram catalyst when the total pressure of the reactant was 400 to 500 mm.-Hg and acetylene content approximately 35%.

From the dependence of the hydrogenation rate of acetylene upon temperature, the activation energies of the reaction on the various carriers were obtained as follows: carbon black 10, French chalk 11, quartz sand 11, powdered active carbon 11, kieselguhr 10, alumina 12 kcal. per mole.

Now we come to consider the experimental data mentioned above to study the functions of the carriers for the various cases.

Consideration

We have observed the various types of the reaction curves in the several figures. Now we shall consider how and why these different types of the reaction can occur by the palladium catalyst on the various carriers and study on the functions of carriers for individual cases.

In the preceding paper several functions of a carrier were referred and it was suggested from the kinetical treatment of the reaction that the dispersity of catalyst has connection with the appearance of various "active regions" of the catalyst surface.

As we see in Fig. 1, in the case of such carriers as carbon black, active carbon (Merck), French chalk and Japanese acid clay, the hydrogenation of acetylene proceeded in two distinct steps quite similarly to the case of kieselguhr or alumina and the hydrogenation of ethylene to ethane could not proceed while acetylene was present in the reactant, because of the strong adsorption of acetylene on the palladium surface.

If the carriers provide only a larger effective surface of the catalyst proper, the ratio of the hydrogenation rate of acetylene to that of ethylene is not to be altered by the carriers, though the rate of the hydrogenations may be changed by them. In fact, the ratio of the two hydrogenation rates changed according to the carriers as shown in Table 1. While the activation energies of the hydrogenation of acetylene showed approximately the same value for the carriers, it may be said from the kinetical treatment that the effective area of the various "active regions" of the catalyst will be changed by the kinds of carriers not only their area, but also the proportions of the individual "active regions."

As shown in Fig. 2, the hydrogenation of acetylene proceeded on the Pd-granular active carbon in a different way from such carriers as alumina or kieselguhr, and the hydrogenations of acetylene and ethylene occurred side by side, not proceeding in two distinct steps. Thus it was shown that the granular active carbon is not to be used as a carrier in practice for the selective hydrogenation of acetylene.

But when the catalyst was powdered in the mortar, the reflection point appeared, at which, as the gas analysis showed, all acetylene was consumed, while the ethane formation was already observed before the point. This fact

shows that the different type of the curve in Fig. 2 is not to be ascribed to the disappearance of the self-retardation of acetylene, but to the heap of the carrier. Hence, it is to be explained as follows: in the case of the granular carrier the rate of diffusion of the reactant or acetylene into the inner part of the granule is not so fast as the reaction rate at the part, the self-retardation of acetylene, therefore, is not to be seen there, being deficient in the gas, and proceeding the ethane formation, while acetylene is present in the bulk space. When the catalyst was powdered, the proportion of the inner part of the granule practically decreased and the ethane formation in the presence of acetylene could not proceed so much as the granular one, while the reflection point appeared somewhat later than the normal carriers. Hence, the self-retardation of acetylene was also to be observed by the experiments as shown in Fig. 3, and when the acetylene content in the initial composition of the reactant was increased, the reaction rate was appreciably retarded as in the case of such carriers as alumina and others.

In the case of Pd-silica gel catalyst the reaction curve was very similar with that of powdered active carbon, suggesting the similar mechanism of the hydrogenation. It is suggested, consequently, that from these reaction curves we can study the structural property of materials, using them as a carrier of this reaction.

When the quartz sand was used as a carrier, the hydrogenation proceeded in a different way from others. As shown in Fig. 4, the ethane and ethylene formations occurred simultaneously, showing no self-retardation of acetylene.

The Pd-quartz sand catalyst was, as it were, a mixture of palladium metal and quartz sand, because of the scanty adsorbability of the carrier and the experiments were not so reproducible as the other carriers, as the distribution of the palladium was not so homogeneous. But it was observed that the initial reaction rate was not so retarded by the increased content of acetylene in the reactant as shown in Fig. 5. The following explanation will possibly be given in this case: scanty adsorbability of the carrier resulted in the much deposited polymers on the surface of the catalyst proper. Hence, the adsorption rate of acetylene was retarded in such an extent that the rate became slower than that of the reaction rate on the catalyst surface. Thus, the effective surface of the catalyst being not covered by acetylene, both hydrogenations of acetylene and ethylene proceeded side by side, showing no self-retardation of acetylene. The considerably fast rate of hydrogenation of acetylene on this catalyst, as given in Table 1, is also considered to support this explanation, as the scanty adsorbability of the carrier should result in the smaller area of the catalyst surface if acetylene covers the catalyst surface as in the other carriers.

Summary

Aceytlene was hydrogenated by palladium deposited on such carriers as carbon black, active carbon (Merck), Japanese acid clay, French chalk, silica gel, granular active carbon, and quartz sand, and the functions of the carriers were considered for individual cases.

The catalysts deposited on the first four carriers catalyzed the hydrogenation in two distinct steps at 30° in the same manner as alumina and kieselguhr, that is, hydrogenation and polymerization of acetylene proceeded in the first step and then ethylene was reduced to ethane in the second step, showing a pronounced self-retardation of acetylene. It was suggested that the kind of carriers has connection with the appearance of various "active regions" with different ratios.

When the granular active carbon was used as a carrier, the hydrogenations of acetylene and ethylene proceeded not in two steps, but simultaneously. This phenomenon was explained by the slow diffusion velocity of acetylene into the inner part of the granule. Powdering the catalyst, the reflection point appeared in the hydrogenation curve and the curve was very similar to that of silica gel, suggesting a similar mechanism of the reaction.

When the quartz sand was used as a carrier, the hydrogenations of the two hydrocarbons occurred at the same time. This is explained by the retardation of the adsorption rate of acetylene by the deposited polymers to such an extent as the adsorption rate becomes to be rate-determining.

It was shown, therefore, that the granular active carbon and quartz sand are not to be used in practice for the selective hydrogenation of acetylene.

The author expresses his sincere thanks to Dr. Sameshima and Dr. H. Akamatu for their kind guidance and encouragement throughout this work.

The expense for the experiments has been defrayed from the Scientific Research Expenditure of the Department of Education.

Department of Chemistry, Faculty of Science, the University of Tokyo, Tokyo

Magnetic Properties of Condensed Aromatic Hydrocarbons with Four Benzene Nuclei. I. On the Diamagnetism of Chrysene

By Hidemasa HONDA and Kōji ŌUCHI

(Received April 28, 1951)

Introduction

The Pascal's additive law[1] of magnetic susceptibility is very well adopted to the aliphatic compounds but the values of molecular susceptibility of aromatic compounds in the treatment as well as the aliphatic compounds for the carbon and hydrogen atoms are diamagnetically smaller than the experimental values. Pascal assigned this excessive parts of diamagnetism to the respective carbon atoms that form the condensed nuclei. Taking into account the constitutive corrections the larger the condensibility of benzene nuclei is, the larger the difference between the calculated values by additive law and the experimental ones becomes.

On the other hand, F. London[2] calculated the ratios of the diamagnetic anisotropies of various condensed aromatic compounds to that of benzene by a quantum mechanical procedure, based on Hückel's molecular orbital treatment, extending to the case of the presence of a magnetic field and obtained an excellent agreement with experiment.

In general, the diamagnetism of condensed aromatic hydrocarbons becomes larger with the increase of hexagon number, but it will be expected that the diamagnetic susceptibilities of condensed aromatic hydrocarbons with the same number of hexagon are changed by the form of molecule. Accordingly, the London's theory is applied to the theoretical calculation of the anisotropic part in the condensed aromatic hydrocarbons with four benzene nuclei and the experimental values are compared.

Form of Chrysene Molecule

The X-ray analysis of chrysene crystal has been made by Iball[3]. The crystal belongs to the space group C_{2h}^6 (12/C) or C_3^4 (1C). The dimensions of the unit cell are $a=6.59$, $b=7.84$, $c=14.17$ Å., $\beta=103.5°$, and it contains 4 molecules. The crystal density 1.27, melting point 250°C., boiling point 448°C., molecular weight 228, and the form of molecule is plane and consists of regular hexagons with interatomic distances of 1.41 Å.

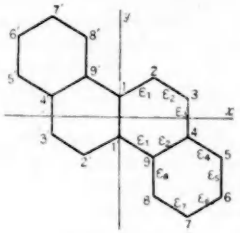

Fig. 1.

Theoretical Calculation

The present calculation follows the same notation and procedure as London's paper.[4] London's secular equation is as follows:

$$|\eta_{kl}\exp(2\pi i f_{kl}) - x\delta_{kl}| = 0, \qquad (1)$$

where $\eta_{kl}\begin{cases}1 & \text{if } k \text{ is a neighbor of } l\\ 0 & \text{if } k \text{ is not a neighbor of } l\end{cases}$

$\delta_{kl}\begin{cases}1 & \text{if } k=l\\ 0 & \text{if } k=l,\end{cases}$

$$f_{kl} = \frac{e}{2hc}H(x_k y_l - x_l y_k), \qquad (2)$$

$$\exp(2\pi i f_{kl}) = W_{kl}/W_1, \qquad (3)$$

and

$$x = \frac{E^{(1)} - W_0}{W_1} \qquad (4)$$

In Eq. (2), H is the field strength, x_k etc. are the coordinates and f_{kl} can be considered as a numerical value proportional to the magnetic flux through the area of the triangle

(1) *Cf.*, for instance, P. W. Selwood, "Magnetochemistry", New York, 1943.
(2) F. London, *J. de Physique*, **8**, 397 (1937).
(3) J. Iball and J. M. Robertson, *Nature*, **132**, 750 (1933); J. Iball, *Proc. Roy. Soc.* (*London*), **A 146**, 140 (1934).
(4) F. London, *J. de Physique*, **8**, 397 (1937).

formed by the neighbors k, l and the origin, arbitrarily chosen in the plane of the molecule. In Eq. (3), W_{kl} represents the exchange integral in the presence of magnetic field and W_1 is the ordinary exchange integral of the nearest neighbors of the orbital theory in the absence of magnetic field. In Eq. (4), $E^{(1)}$ is the ordinary first order perturbation energy and W_0 is the Coulomb integral independent of the magnetic field.

Following the above conditions and the model shown in Fig. 1, the following secular determinant of chrysene molecule can be gained.

$$
\begin{array}{c|cccccccccccccccccc|}
 & 1 & 2 & 3 & 4 & 5 & 6 & 7 & 8 & 9 & 1' & 2' & 3' & 4' & 5' & 6' & 7' & 8' & 9' \\
\hline
1 & -x\varepsilon_1 & & & & & & & & & 1 & & & & & & & \varepsilon_1^* \\
2 & \varepsilon_1^* & -x\varepsilon_2 & & & & & & & & & & & & & & & & \\
3 & & \varepsilon_2^* & -x\varepsilon_3 & & & & & & & & & & & & & & & \\
4 & & & \varepsilon_3^* & -x\varepsilon_4 & & & & & & & & & & & & & & \\
5 & & & & \varepsilon_4^* & -x\varepsilon_5 & & & & & & & & & & & & & \\
6 & & & & & \varepsilon_5^* & -x\varepsilon_6 & & & & & & & & & & & & \\
7 & & & & & & \varepsilon_6^* & -x\varepsilon_7 & & & & & & & & & & & \\
8 & & & & & & & \varepsilon_7^* & -x\varepsilon_8^* & & & & & & & & & & \\
9 & & & & \varepsilon_2^* & & & & \varepsilon_8 & -x\varepsilon_1 & & & & & & & & & \\
1' & 1 & & & & & & & & & \varepsilon_1^* & -x\varepsilon_1 & & & & & & & \\
2' & & & & & & & & & & & \varepsilon_1^* & -x\varepsilon_2 & & & & & & \\
3' & & & & & & & & & & & & \varepsilon_2^* & -x\varepsilon_3 & & & & & \\
4' & & & & & & & & & & & & & \varepsilon_3^* & -x\varepsilon_4 & & & \varepsilon_2 & \\
5' & & & & & & & & & & & & & & \varepsilon_4^* & -x\varepsilon_5 & & & \\
6' & & & & & & & & & & & & & & & \varepsilon_5^* & -x\varepsilon_6 & & \\
7' & & & & & & & & & & & & & & & & \varepsilon_6^* & -x\varepsilon_7 & \\
8' & & & & & & & & & & & & & & & & & \varepsilon_7^* & -x\varepsilon_8^* \\
9' & \varepsilon_1 & & & & & & & & & & & & & & & & \varepsilon_2^* & \varepsilon_8 - x \\
\hline
\end{array} = 0, \qquad (5)
$$

where $\varepsilon_k = \exp(2\pi i f_{k,k+1})$

and $\varepsilon_k^* = \exp(-2\pi i f_{k,k+1})$.

For convenience' sake, ε_k is preferred to ε_k^* in case of the clockwise rotation about the origin.

This secular determinant can be transformed to the type as follows:

$$
\begin{vmatrix} \Delta_1 & 0 \\ 0 & \Delta_2 \end{vmatrix} = 0.
$$

Therefore Eq. (5) can be separated into the solution of two determinants, namely

$$
\Delta_1 = \begin{array}{c|ccccccccc|}
 & 1 & 2 & 3 & 4 & 5 & 6 & 7 & 8 & 9 \\
\hline
1 & (1-x)\varepsilon_1 & & & & & & & & \varepsilon_1^* \\
2 & \varepsilon_1^* & -x\varepsilon_2 & & & & & & & \\
3 & & \varepsilon_2^* & -x\varepsilon_3 & & & & & & \\
4 & & & \varepsilon_3^* & -x\varepsilon_4 & & & & & \varepsilon_2 \\
5 & & & & \varepsilon_4^* & -x\varepsilon_5 & & & & \\
6 & & & & & \varepsilon_5^* & -x\varepsilon_6 & & & \\
7 & & & & & & \varepsilon_6^* & -x\varepsilon_7 & & \\
8 & & & & & & & \varepsilon_7^* & -x\varepsilon_8^* & \\
9 & \varepsilon_1 & & & \varepsilon_2^* & & & & \varepsilon_8 - x & \\
\hline
\end{array} = 0
$$

and

$$
\Delta_2 = \begin{array}{c|ccccccccc|}
 & 1 & 2 & 3 & 4 & 5 & 6 & 7 & 8 & 9 \\
\hline
1 & (-1-x)\varepsilon_1 & & & & & & & & -\varepsilon_1^* \\
2 & \varepsilon_1^* & -x\varepsilon_2 & & & & & & & \\
3 & & \varepsilon_2^* & -x\varepsilon_3 & & & & & & \\
4 & & & \varepsilon_3^* & -x\varepsilon_4 & & & & & \varepsilon_2 \\
5 & & & & \varepsilon_4^* & -x\varepsilon_5 & & & & \\
6 & & & & & \varepsilon_5^* & -x\varepsilon_6 & & & \\
7 & & & & & & \varepsilon_6^* & -x\varepsilon_7 & & \\
8 & & & & & & & \varepsilon_7^* & -x\varepsilon_8^* & \\
9 & -\varepsilon_1 & & & \varepsilon_2^* & & & & \varepsilon_8 - x & \\
\hline
\end{array} = 0.
$$

Expanding Δ_1 and Δ_2, and after substitution of ε by f, we have

$$
\Delta_1 = x^9 - x^8 - 10x^7 + 8x^6 + 32x^5 - 21x^4 - 39x^3 + 22x^2 + 15x - 8 + (x^4 + x^3 - 4x^2 - 2x + 6)(2\pi f)^2 = 0 \qquad (6)
$$

and

$$
\Delta_2 = x^9 + x^8 - 10x^7 - 8x^6 + 32x^5 + 21x^4 - 39x^3 - 22x^2 + 15x + 8 - (x^4 - x^3 - 4x^2 + 2x + 6)(2\pi f)^2 = 0, \qquad (7)
$$

where $f = (e/hc) \cdot H \cdot S_B$, $\qquad (8)$

S_B = the area of each hexagon.

Since Eqs. (6) and (7) have the form:

$$
F_1(x) + F_2(x) \cdot (2\pi f)^2 = 0 \qquad (9)
$$

and f is very small, the second term may be considered as a correction. Accordingly, let x' be a root of $F_1(x) = 0$ and

$$
x = x' + x''(2\pi f)^2 \qquad (10)
$$

be a root of Eq. (9), x'' will be expressed approximately by

$$
x'' = \frac{F_2(x')}{F_1'(x')} \qquad (11)
$$

according to Newton's equation. In Eq. (11),

F_1' represents the first differential of F_1 with regard to x.

Now we need nine roots of lower energy levels in eighteen roots of Eqs. (6) and (7). These values are shown in Table 1.

Table 1

$-x'$	x''
2.49904	+0.03965
2.16651	−0.00899
1.70076	−0.12892
1.53977	+0.06547
1.28577	+0.16687
1.21644	−0.29292
0.87532	+0.35968
0.79233	−0.58089
0.52013	+0.62639
Σ;	+0.24638

Substituting the values of x in Eq. (4), $E^{(1)}$ is given and a susceptibility contribution of a π-electron becomes

$$\chi_p = -\left(\frac{\partial^2 E^{(1)}}{\partial H^2}\right)_{H\to 0} \qquad (12)$$

From (4), (8), (10), (12) and numerical value of $\sum(x'')$ we obtain the diamagnetic anisotropy of chrysene as follows:

$$\Delta\chi = 2\sum_{p=-\frac{N-2}{4}}^{\frac{N-2}{4}} \chi_p = -4\sum(x'')\,|W_1|\left(\frac{2\pi e S_B}{hc}\right)^2$$
$$= 18\sum(x'')\Delta\chi_{\text{Benz.}}$$
$$= 4.43\,\Delta\chi_{\text{Benz.}}, \qquad (13)$$

where $\Delta\chi_{\text{Benz.}}$ is the anisotropic contribution of π-electrons in benzene.

Magnetic Measurements and Discussion

The principal diamagnetic anisotropies along the three principal axes of chrysene single crystal have been measured by K. Lonsdale and K. S. Krishnan.[5] These values are as follows:

$$K_1 = -88.0\times10^{-6},\ K_2 = -83.3\times10^{-6},$$
$$K_3 = -310.8\times10^{-6},$$

then the anisotropic part per mole becomes

$$\Delta\chi = 4.17\cdot\Delta\chi_{\text{Benz.}} \qquad (14)$$

We measured the mass susceptibility of powdered chrysene by the modified Gouy's method[6] and chose the purified water as standard. This chrysene specimen had been extracted from coal-tar and purified by several recrystallizations and sublimations. The results obtained as follows:

$$\chi_g = -0.731\times10^{-6},\quad \chi_M = -166.67\times10^{-6},$$

where χ_g and χ_M denote the mass and mole susceptibilities respectively. Accordingly, we can deduce $\Delta\chi$ as follows:

$$\Delta\chi = 4.10\cdot\Delta\chi_{\text{Benz.}}, \qquad (15)$$

using the modification of Pascal's additive law.[7]

This result (Eq. (15)) coincides closely with that of relation (Eq. (14)), and the result calculated according to London's theory (Eq. (13)) shows a relatively good agreement with the experiments.

The difference of K_1 and K_2 in chrysene is small but, in general, it is expected that the larger the discrepancy of molecular form from the circle is, the larger this difference becomes. Accordingly, the relative diamagnetic anisotropies to benzene under the assumption of $K_1 = K_2$ will become uncertainly, then it may be doubtful to compare the values of experimental relative anisotropy to the theoretical values. These questions have to be discussed further in detail.

In this experiment, the electromagnet was lent to the authors by the Glass Research Institute, Tohoku University, and they wish to express their sincere thanks to Prof. Hitoshi Tominaga and Prof. Genjiro Hazato, for their kind permisson and advice.

The authors thanks are also due to Mr. Saburo Fujii, who belongs to Tokyo Institute of Technology, for his enthusiastic discussion, and Mr. Sugiya Fujii, the staff of our institute, for his generosity in providing the chrysene sample.

Nenryo-Kenkyusho (Fuel Research Institute)
Kawaguchi, Saitama Pref.

(5) K. Lonsdale and K. S. Krishnan, *Proc. Roy. Soc. (London)*, **A 156**, 597 (1936); K. Lonsdale, *Proc. Roy. Soc. (London)*, **A 159**, 149 (1937).

(6) *Cf.*, for example, P. W. Selwood, "Magnetochemistry," New York (1943); G. Hazato and K. Aida, *Rep. Glass Research Institue, Tohoku Univ.*, No. 3 (1949).

(7) G. Hazato, *J. Chem. Soc. Japan*, **64**, 483 (1943); H. Shiba and G. Hazato, This Bulletin, **22**, 92 (1949).

Heterogeneous Hydrolytic Degradation of Cellulose

By Kei MATSUZAKI and Hiroshi SOBUE

(Received May 1, 1951)

Introduction

As it is well-known, cellulose is a chain molecule consisted of glucosidic anhydrides linked together through 1- and 4-positions. Recently, E. Husemann[1] investigated hydrolysis of purified ramie in 0.5 *M* $KHSO_4$ solution for 2-1200 hours at 60°. Chain length distribution of the nitrates of both slightly and extremely hydrolyzed products indicated a uniform splitting of the glucosidic bonds, but the chain length distribution of intermediately hydrolyzed products showed an increase in uniformity especially in the products of a degree of polymerization (D. P.) of 400-500. He concluded that wood cellulose as well as cotton and ramie cellulose has weak bonds at intervals of about 500 glucose units which split 5000 times faster than the usual glucosidic bonds. G. V. Schulz[2] also stated the same conclusion and the others supported him. Since 1946, E. Pacsu[3] suggested the presence of hemiacetal bonds at intervals of 260 glucose units which split on mild hydrolysis faster than the usual glucosidic bonds. E. Heuser,[4] according to his unpublished work, also found that a uniform splitting took place upon hydrolysis of cotton cellulose in H_3PO_4, but of Aspen wood cellulose, molecules of a chain length of about 500 glucose units were accumulated, as Schulz *et al.* recognized.

If cellulose has such acid-weak bonds in its linkages, and cellulosic materials are submitted to acid treatments such as sulphite cooking, acetylation or nitration, the chain length distribution of the samples treated should be different from the case where uniform splitting takes place. We showed, in our previous work,[5] that the fractional precipitation of cellulose nitrate with acetone-ligroin gave superior results to that of fractional solution with acetone-ethanol or ethyl acetate-ethanol, or fractional precipitation with acetone-water. The distribution becomes broad and it seems that high-molecular as well as low-molecular fractions are considerably separated enough. We applied this fractional procedure to purified cotton, wood cellulose and heir hydrolyzed products and attempted to prove the presence of the weak bonds and investigated heterogeneous hydrolysis of cellulose as a model experiment of cooking.

Experimental Procedures and Results

Samples studied were purified surgery cotton and red pine (Pinus densiflora S. *et* Z.) pulp for viscose rayon grade. 4 g. of conditioned samples were weighed and imbibed in 300 cc. of 3.5 *N* HCl for 4-120 hours at 30°. At the end of each specified hydrolysis period, they were taken out, washed thoroughly, dried in air and then dried under vacuum in $CaCl_2$ desiccator. Table 1 shows

Table 1

Results of Heterogeneous Hydrolysis of Cotton and Wood Pulp in 3.5 *N* HCl at 30°

Time	Purified Cotton Residue, %	D. P.	Wood Pulp Residue, %	D. P.
0	—	1080	—	950
4	99.7	889	—	—
24	99.1	466	98.8	488
48	—	—	98.7	400
72	98.9	318	98.5	343
120	98.7	282	98.3	321

the weight loss and D. P. change of the samples by these mild hydrolysis. In spite of the large changes in D. P. the weight loss is very little, because of recrystallization[6] of splitted, disorganized and strained chains. Then these degraded samples were nitrated with the acid mixtures of HNO_3, H_3PO_4 and P_2O_5 (60:35:5) for 6 hours at 0°. The nitrates were washed with water for 24 hours and stabilized with methanol refluxing for 30 minutes. About 2 % of methanol soluble products were obtained. As nitrogen content and viscosity of the stabilized products increased with this treatment, the methanol

(1) E. Husemann, *Makromol. Chem.*, **1**, 140 (1947); E. Husemann and M. Goecke, *ibid.*, **2**, 293 (1948); **4** 194 (1949).
(2) G. V. Schulz and G. Sing, *J. Polymer Sci.*, **3**, 385 (1948).
(3) P. C. Mehta and E. Pacsu, *Textile Research J*, **18**, 387 (1948).
(4) E. Heuser, Tappi, Monograph Series No. 6, 8-74 (1948).
(5) K. Matsuzaki and H. Sobue, *J. Chem. Soc. Japan, Ind. Chem. Sec.*, **54**, 289 (1951).
(6) O. A. Battista, *Ind. Eng. Chem.*, **42**, 507 (1950); J. A. Howsmon, *Textile Research J.*, **19**, 152 (1949).

soluble products would probably have low nitrogen content and low D. P. Also, almost all of combined H_3PO_4 is removed by this treatment. Acetone solution (1%) of the stabilized nitrates was then fractionally precipitated with ligroin and the weight and D. P. of each fraction were determined. The results are tabulated in Tables 2-9.

As a number of samples have high molecular weight, high-molecular fractions were at first precipitated, dissolved in acetone again and re-fractionated. Integral chain length distribution curves were plotted and by graphical differentiation differential chain length distribution curves were also plotted. The curves are illustrated in Figs. 1-4.

Since two main fractions were separately fractionated for a number of samples, integral and differential distribution curves should be obtained from the summation of the curves for the two main fractions. But, as the procedure which enables to obtain continuous integral curves from the step-wise experimental data contains an arbitrary factor, we plotted integral curves for these samples simply rearranging all fractions in the order of D. P. without plotting the curves for the two main fractions separately.

Table 2

Fractionation of Nitrate of Purified Cotton. Sample 5.002 g., Yield 97.3%. av. D. P. 1080, N 12.86%(7)

High-molecular Fractions			Low-molecular Fractions		
Fraction	Weight %	D. P.	Fraction	Weight %	D. P.
1	2.20	500	1	2.91	90
2	0.78	910	2	1.31	140
3	12.76	935	3	2.68	230
4	1.80	1085	4	5.37	335
5	5.88	1160	5	3.54	495
6	2.32	1255	6	3.31	595
7	8.24	1465	7	2.58	680
8	2.60	1580	8	12.44	750
9	11.20	1605	9	3.19	1205
10	7.43	1740	total	37.33	
11	7.43	1950			
total	62.64				

Table 3

Fractionation of Nitrate of 4-hrs. Hydrolyzed Purified Cotton. Sample 5.004 g., Yield 96.3%, av. D. P. 889, N 13.09%

High-molecular Fractions			Low-molecular Fractions		
Fraction	Weight %	D. P.	Fraction	Weight %	D. P.
1	2.10	290	1	4.53	95
2	1.15	340	2	5.25	160
3	0.72	410	3	2.66	215
4	1.18	535	4	6.30	275
5	8.50	560	5	5.42	360
6	4.90	790	6	4.39	445
7	16.36	850	7	5.67	480
8	1.99	885	8	13.05	630
9	4.28	1050	9	3.38	820
10	1.52	1075	10	2.69	1005
11	3.96	1330	total	53.34	
total	46.66				

(7) Details of the fractional procedures are given in the following issue: *The Science of Forest Products*, **5**, 53 (1950).

Table 4

Fractionation of Nitrate of 24-hrs. Hydrolyzed Purified Cotton. Sample 3.030 g., Yield 97.2%, av. D.P. 466, N 12.96%

Fraction	Weight %	D. P.
1	6.17	75
2	1.65	160
3	3.99	170
4	3.76	190
5	3.91	210
6	10.57	280
7	3.70	345
8	0.74	345
9	7.07	365
10	15.71	430
11	5.76	490
12	12.36	675
13	19.88	750
14	4.73	885

Table 5

Fractionation of Nitrate of 72-hrs. Hydrolyzed Purified Cotton. Sample 3.051 g., Yield 97.2%, av. D. P. 318, N 13.1%

Fraction	Weight %	D. P.
1	10.58	55
2	1.17	110
3	5.74	130
4	4.32	155
5	7.41	200
6	1.56	230
7	13.70	245
8	1.81	300
9	3.35	315
10	5.93	330
11	13.41	340
12	6.41	430
13	17.80	535
14	6.81	630

Table 6

Fractionation of Nitrate of 120-hrs. Hydrolyzed Purified Cotton. Sample 3.048 g., Yield 96.3%, av. D. P. 282, N 12.93%

Fraction	Weight %	D. P.
1	9.76	45
2	1.28	115
3	7.71	130
4	3.62	155
5	5.94	175
6	1.27	215
7	13.83	235
8	1.43	290
9	2.59	300
10	5.42	305
11	17.13	320
12	6.24	400
13	15.26	480
14	8.53	620

Table 7

Fractionation of Nitrate of Wood Pulp. Sample 5.056 g., Yield 95.3%, av. D. P. 950, N 12.9%

Fraction	Weight %	D. P.
1	4.84	2360
2	8.11	2020
3	4.17	1910
4	9.16	1720
5	5.15	1630
6	9.82	1170
7	8.67	1010
8	2.11	690
9	15.77	545
10	1.74	425
11	2.92	335
12	5.44	295
13	10.77	170
14	11.36	45

Table 8

Fractionation of Nitrate of 48-hrs. Hydrolyzed Wood Pulp. Sample 2.869 g., Yield 95.0 %, av. D.P. 400, N 12.9%

Fraction	Weight %	D. P.
High-molecular Fractions		
1	6.77	1095
2	3.05	950
3	2.65	820
4	8.83	650
Low-molecular Fractions		
1	0.97	940
2	9.03	555
3	6.60	480
4	16.50	370
5	16.63	305
6	9.71	170
7	8.18	80
8	5.07	80
9	2.51	40
10	3.50	—

Table 9

Fractionation of Nitrate of 120-hrs. Hydrolyzed Wood Pulp. Sample 2.805 g., Yield 95.8 %, av. D.P. 321, N 12.9 %

Fraction	Weight %	D. P.
High-molecular Fractions		
1	2.05	920
2	3.88	735
3	6.51	530
Low-molecular Fractions		
1	0.77	720
2	6.92	415
3	5.03	385
4	12.63	300
5	22.07	270
6	7.13	230
7	7.27	140
8	7.15	105
9	18.59	30

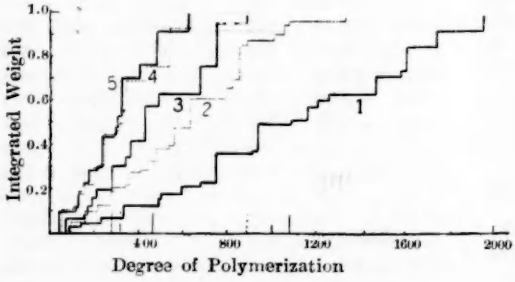

Fig. 1.—Integral chain length-weight distribution curves of hydrolyzed cotton (3.5 *N* HCl, 30°): 1, original; 2, 4 hrs. hydrolyzed; 3, 24 hrs. hydrolyzed, 4, 72 hrs. hydrolyzed, 5, 120 hrs. hydrolyzed

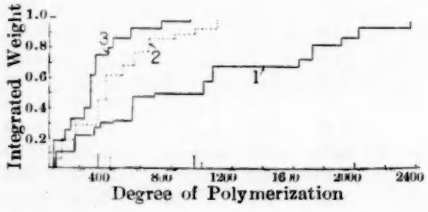

Fig. 2.—Integral chain length-weight distribution curves of hydrolyzed wood pulp (3.5 *N* HCl, 30°): 1, original; 2, 48 hrs. hydrolyzed; 3, 120 hrs. hydrolyzed.

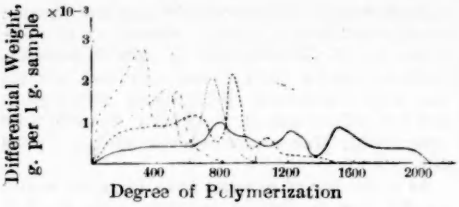

Fig. 3.—Differential chain length-weight distribution curves of hydrolyzed cotton: —— original; ---- 4 hrs. hydrolyzed; ..... 24 hrs. hydrolyzed, ----- 120 hrs. hydrolyzed.

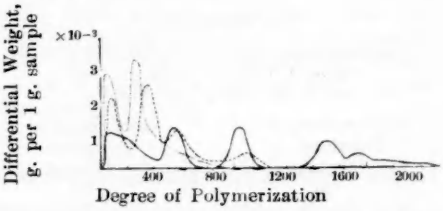

Fig. 4.—Differential chain length-weight distribution curves of hydrolyzed wood pulp: —— original; ---- 4 hrs. hydrolyzed; ..... 120 hrs. hydrolyzed.

Discussion

From Figs. 1-4, the difference between the chain length distributions of purified cotton and wood cellulose is evident, although these two samples have been degraded with several purification treatments. Wood cellulose has more low and high molecular weight fractions and more nonuniform distribution of chain length than purified cotton. The difference does not disappear even if the hydrolysis proceeds. The weight loss is little due to recrystallization and it is evident that the short recrystallized splitted chains are also included in the samples. These short chains of lower D. P. than 200 increase rapidly, as hydrolysis proceeds. Several maxima in the chain length distribution curves of purified cotton and pulp shifts to low molecular weight as the reaction proceeds. It seems as if these maxima are not so distinct as to give a positive proof of the presence of the weak bonds which would split 5000 times faster than the usual bonds and exist at regular intervals of 500 or 260 glucose units. If those acid-sensitive bonds exist in cellulose molecules, more rapid accumulation of chains of 500 or 260 glucose units would be expected. The heterogeneous degradation of cellulose can be explained well with its submicroscopic structure as follows.

In cotton and wood cellulose, crystalline

regions of relatively uniform length exist between amorphous regions. On hydrolysis, acid diffuses into the amorphous regions where the chains are splitted. Therefore the D. P. becomes lower and lower as the hydrolysis proceeds giving rise to several maxima in the differential distribution curves corresponding to several times the length of crystalline regions. Chain length of the crystalline regions at the beginning of the hydrolysis seems to be 200-300. Although the reason for the discrepancy between this value and that measured with x-ray method (120) is not yet clear, it is probable that the chain length of the crystalline regions grows long by the recrystallization of the splitted chains or acid-resistant crystalline regions may have different D. P. from that determined with x-ray method.

As previously mentioned, the nonuniformity of chain length distribution of wood pulp does not disappear upon hydrolysis. This indicates that the submicroscopic structure of wood pulp is not uniform. On one side, its amorphous regions are easily attacked with acid, but on the other, the crystalline regions or mesomorphous regions are more resistant to acid than that of cotton. This nonuniformity of crystalline structure of wood pulp would be closely related with the difference in chain length distribution and reactivity of cotton when submitted to micellar reactions as hydrolysis, xanthation or acetylation.

Summary

Purified cotton and wood pulp were hydrolyzed in 3.5 *N* HCl for 4-120 hours at 30°. The hydrolyzed products were nitrated with the mixtures of H_3PO_4-HNO_3-P_2O_5 at 0° for 6 hours. Acetone solutions of the nitrates were fractionally precipitated with ligroin, and chain length distribution curves were plotted. These curves show no positive proof of the presence of the weak bonds which split 5000 times faster than the usual glucosidic bonds. These are well explained with the submicroscopic structure of cellulose.

The authors express thanks to Kazuo Kosuge and Takeo Iwata for their earnest aids to the experiment. The expense of this work was defrayed from the Scientific Research Encouragement Grant of the Department of Education.

Department of Applied Chemistry, Faculty of Engineering, the University of Tokyo, Tokyo

The Absorption Spectra of Quinolino-quinolines

By Kazuo SHIBATA

(Received May 10, 1951)

The recent advances in chemical physics have enabled us to interpret the electronic states and spectra of rather complicated molecules, although the theoretical treatments are more or less crude ones, which may be inevitable at the present stage of our knowledge. In this respect, the most well studied are aromatic hydrocarbons, while no pertinent investigations have hitherto been made with hetero-molecules, which is mainly due to the lack of spectroscopic data on these substances. The present report is concerned with the study of spectroscopic properties of quinolino-quinoline compounds, with a view to contributing fundamental data for theoretical elucidation of electronic states of heterocyclic compounds.

The compounds investigated were the following four types of quinolino-quinolines;

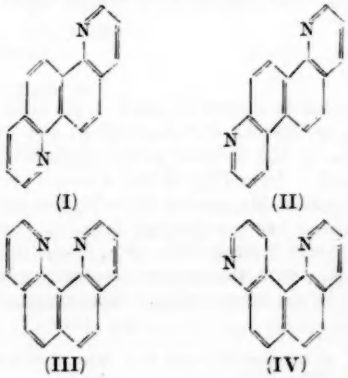

Among these, the componds (I) and (II) correspond to the hydrocarbon chrysene, and (III) and (IV) to 3, 4-benzo-phenanthrene. The solvent used was ethanol and the measurement of absorption was made within the range of 2500 Å. to 4000 Å. by using the quartz-spectrograph QM-60 combined with the photo-multiplier-tube 1P28.

It was found that the four compounds studied have the property in common of showing three main absorption bands, among which the band at the shortest wave-length is most intensive, while the other two have almost the same intensity. These three bands may be regarded as corresponding to the three bands of chrysene and 3, 4-benzo-phenanthrene, respectively. The characteristic features of the absorption bands shown by quinolino-quinolines lie in the fact that, in the case of the compounds (I) and (II), the second band is split into two, while in the case of compounds (III) and (IV) the splitting occurs in the band at the longest wave-length. The absorption maxima observed are listed in Table 1, in which also the data for chrysene and 3, 4-benzo-phenanthrene reported by Klevens and Platt[1] are given for comparison.

Table 1 (λ in Å. unit)

Compounds	First band	Second band	Third band
Chrysene	2690	3310	3640
I	2640	2940, 3080	3490
II	2650	2930, 3060	3490
III	2640	3100	3460, 3610
IV	2690	3050	3460, 3660
3, 4-benzo-phenanthrene	2810	3300	3740

As may be seen from the table, the absorption spectra shown by the compounds (I) and (II) are very similar to each other, resembling on the whole the spectrum shown by chrysene, while those of compounds (III) and (IV) are similar to each other, both resembling the spectrum of 3, 4-benzo-phenanthrene. It is, however, to be noticed that when compared with bands shown by the corresponding hydrocarbons, the bands shown by quinolino-quinolines are always shifted more or less to the side of shorter wave-lengths. At any rate, it may be concluded that the replacement by nitrogen of the carbon in a benzene ring entails far less change in the spectroscopic properties of aromatic compounds than does the change in the mode of combination of benzene nuclei.

The author wishes to express his thanks to Prof. E. Ochiai for giving the author his precious compounds for this research.

(1) H. B. Klevens and J. R. Platt, *J. Chem. Phys.*, **17**, 470 (1949).

Tokugawa Institute for Biological Research, Tokyo

The Absorption Bands of Benzene and Its Derivatives in Visible Region

By Kazuo SHIBATA, Hiroshi KUSHIDA and Seiyō MORI

(Received May 10, 1951)

Benzene is known to show four absorption bands at 1850 Å., 2070 Å., 2590 Å. and 3400Å., the one at the shortest wave-length being the strongest. According to the theory proposed by Goeppert-Mayer and Sklar[1], the molecule of benzene has one ground level $^1A_{1g}$ and six lower excited levels $^3B_{1U}$, $^3E_{1U}$, $^3B_{2U}$, $^1B_{2U}$, $^1B_{1U}$ and $^1E_{1U}$, with the energies increasing progressively in the given order. The strongest absorption band at 1850 Å. was attributed to the transition $^1A_{1g}-{}^1E_{1U}$, and the bands at 2070 Å. and 2590 Å. were ascribed to the transition $^1A_{1g}-{}^1B_{1U}$ and $^1A_{1g}-{}^1B_{2U}$, respectively. As to the band at 3400 Å., an interpretation was given in the paper of the authors named, but later it was assumed by Sklar[2] to be due to the forbidden $^1A_{1g}-{}^3E_{1U}$ transition. This theory, however, cannot be regarded as being quite satisfactory, especially in so far as it restricts

(1) M. Goeppert-Mayer and A. L. Sklar, *J. Chem. Phys.*, **6**, 645 (1938).

(2) A. L. Sklar, *Rev. Mod. Phys.*, **14**, 232 (1942).

the considerations only to the transition to the triplet states. Indeed, it has been criticized by London,[3] Mulliken[4] and Shull[5] from various points of view; but even when we take into account the opinions of these authors, we cannot explain why the singlet-triplet transition would not yield the corresponding absorption bands, which may lie in the visible region. Apart from these considerations, it seemed worth while to scrutinize the spectroscopic properties of benzene and its derivatives in the visible region. It was found that, besides the four bands hitherto known, benzene and some of its derivatives show a weak, but distinct, absorption band in the vicinity of 5200-5300 Å., which, strangely enough, has escaped observations by the earlier workers.

The measurements were made by photoelectric method, using a multiplier photo-tube RCA 931 A. The samples were purified by the method described in "Organic Solvent"[6] with the greatest possible care. The observations were made with a pure substance without using any solvent. The thickness of the liquid in the cell was 20 cm.

The maximum of the band shown by benzene was situated at 5200 Å. with the intensity of about 5×10^{-6} in molar extinction coefficient unit. The corresponding absorption was also found in toluene, monochlorobenzene and tetralin with the maximum at 5290 Å., 5250 Å. and 5280 Å., respectively. In the cases of benzene, monochlorobenzene and tetralin, the curves of absorption spectrum showed a smooth protrusion in the said spectral region, while that of toluene was split into two crests. It may be reasonable to assume that these bands are due to the singlet-triplet transitions, although the numerical agreement, with the calculated energy difference found in earlier reports, is not satisfactory.

In addition to the new finding described above, it is of great interest to note that there is a nice simple rule governing the location of absorption bands observed in benzene. Namely, if we divide the wave-numbers (in cm^{-1} unit) corresponding to the absorption maxima with 9653 cm^{-1}, we obtain almost the round numbers 2, 3, 4 and 5, except for the band at 1850 Å. which gave the figure 5.6 (see Table 1). We

Table 1

λ in Å.	ν in cm^{-1}	1/9653
1850	54054	5.600
2070	48356	5.009
2590	38612	4.000
3400	29412	3.047
5200	19231	1.992

are not in a position at present to give an explanation of this interesting rule, but it is doubtless that it involves a problem which awaits theoretical elucidation in the future.

Tokugawa Institute for Biological Research, Tokyo

(3) A. London, *J. Chem. Phys.*, **13**, 396 (1945).
(4) R. S. Mulliken, *J. Chem. Phys.*, **16**, 118 (1948).
(5) Shull, *J. Chem. Phys.*, **17**, 295 (1949).
(6) A. Weissberger and E. Proskauer, "Organic Solvents."

A Remark on the Goeppert-Mayer and Sklar's Theory on the Excited States of Benzene

By Kazuo SHIBATA

(Received May 10, 1951)

Of the numerous theoretical procedures which have been proposed to elucidate the electronic states of benzene, the most outstanding is the so-called GMS-method (Goeppert-Mayer and Sklar's method), though it is in many respects open to criticism. Despite the effort of London[1] and Mulliken[2] to improve the method, the fundamental deficiency of the theory still remains, especially as it concerns the singlet-triplet transitions. In a preceding paper we have reported that benzene shows an absorption band at 5200 Å, which has been overlooked by

(1) A. London, *J. Chem. Phys.*, **13**, 396 (1945).
(2) R. S. Mulliken, *J. Chem. Phys.*, **16**, 118 (1948).

earlier workers. The purpose of the present paper is to achieve, applying the principle of the GMS-method and taking duly into account the newly discovered absorption band, a more satisfactory agreement of the theory with experimental data. It may be stated in advance that our trial also proved to be far from successful, but its presentation here may be relevant, since it seems to have revealed the limit of applicability of the GMS-method.

To begin with, a correction had to be made in the values of integrals used by Goeppert-Mayer and Sklar[3], which was taken from the Bartlett's table of molecular integrals. We calculated these values by using equations derived by Kotani[4] and Parr and Crawford[5], which gave results coinciding satisfactorily with each other. This agreement may indicate the validity of the recalculated values. Applying the corrected values, the energy differences between the ground level and the excited levels were calculated according to the GMS-method.

For the sake of simplicity, we shall omit here the procedures of calculation and only show the result in Table 1, in which the energy differences are given in e. v. unit.

Table 1

	$^3B_{1U}$	$^3E_{1U}$	$^3B_{2U}$	$^1B_{2U}$	$^1B_{1U}$	E_{1U}
corrected values	0.7	1.3	1.9	3.8	4.3	6.6
uncorrected values	1.5	2.2	3.0	5.0	5.8	8.0

As is indicated by the figures in the table, our corrected values yielded results which are rather in worse agreement with experiments than in the case of the original calculation by Goeppert-Mayer and Sklar. Our calculation gives lower values for all energy levels, and especially so for the triplet states.

The most prominent characteristics of the calculation by GMS-method is that the energy levels can be calculated, though with rather crude approximation, almost absolutely; that is to say, with no parameters and empirical data except those concerning the C-C distance and the effective nuclear charge. Since, however, this method gives such a poor agreement with experiment as shown above, it seems worth while to introduce a parameter in the calculation in order to get better quantitative agreement with the experiment.

In the above calculation, the C-C distance was taken to be $r=1.39$ Å. which was based on the experimental data on benzene. It is, therefore, unreasonable for us to take the value of the C-C distance as a parameter. On the other hand, the effective nuclear charge was chosen to be $Z=3.18$, a value which was obtained by Zener[6] on the basis of a variational calculation minimizing the energy of the ground state of one carbon atom. There is, however, no evidence that the value of Z fitted for the atomic state must be the same as the value for the molecular state. It is to be supposed that the 2p electron cloud of a carbon atom is deformed in the benzene molecule on account of various kinds of interaction. Considering these points, it seems pertinent to take the effective nuclear charge as a parameter. Calculation was made taking the figures 2.28, 3.04, 3.18 and 3.80 as the value of Z. These values were chosen only for the sake of easiness of calculation. The result of the calculation is shown in Fig. 1, in which the height of energy levels is plotted against the values of Z, and the dotted lines show the height of energy levels determined from experiments.

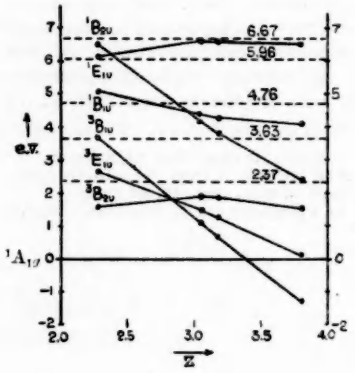

Fig. 1.

It is obvious from this figure that the increase of the value of Z causes the height of energy levels to be lowered, although the heights of $^1E_{1U}$ and $^3B_{2U}$ are not altered profoundly. The heights of excited levels at $Z=3.80$ are not reasonable, because they are too low; equally unreasonable is the result at $Z=2.28$, which does not agree with experiments even qualitatively. Contrary to our expectation, a comparatively better result was obtained at $Z=3.18$, the value that has been used in the original work of Goeppert-Mayer and Sklar. As will

(3) M. Goeppert-Mayer and A. L. Sklar, *J. Chem. Phys.*, **6**, 645 (1938).

(4) M. Kotani, *Proc. of the physico-mathematical Soc. of Japan*, 20, extra No. (1938); **22**, extra No. (1940).

(5) Parr and Crawford, *J., Chem. Phys.* **16**, 1049 (1948).

(6) Zener, *Phys. Rev.*, **36**, 51 (1930).

be seen from these results, our trials to get more satisfactory results than the already obtained one have, on the whole, proved to be quite unsuccessful. The failure we have experienced may show that for attaining satisfactory results we have to improve fundamentally the method of approximation itself.

The author wishes warmly, at this opportunity, to thank Prof. Kotani for his valuable advice and his kind interest in the course of this work.

Tokugawa Institute for Biological Research, Tokyo

Some Rheological Measurements on Coal Tar Pitches[1]

By Tsurutaro NAKAGAWA

(Received May 2, 1951)

Rheological properties of coal tar pitches in the softening range (80°~110°) were studied from the following three points of view. (1) They are used as a binding material for the production of some carbonaceous matter, *e. g.*, carbon brush etc., and their practical quality is said to be partly related to the rheological properties of the binder. (2) Highly viscous substances usually behave as visco-elastic, *i. e.*, they have some elastic nature besides being viscous. Rheological anomalies of these substances may be ascribed to the visco-elastic effects. (3) Internal structure of some bituminous solid, *e. g.*, pitches, asphalts and coals, makes an interesting problem in the present stage of chemistry of coal. Analysis of rheological data may disclose some one of these points.

Experimental

As the experimental procedure for studying and analysing rheological behavior of tar pitches, the author took the method of measuring the visco-elastic properties of the material, using a newly constructed dynamic apparatus suitable for the study in the range of seconds~minutes of period, which should give information about the dynamic modulus and dynamic viscosity much different from those in the audiofrequency range, where much more work has been done.

Dynamic Method for Measuring Visco-elastic Properties. Method by the Phase Difference.[2] — Consider a modification of a rotation viscometer (Fig. 1), and apply the sinusoidal torsional displacement,

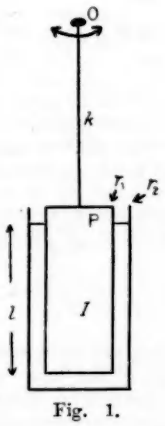

Fig. 1.

$$\Theta = \Theta_0 \sin \omega t ,$$

at the top O of the torsion wire whose torsion constant is k dyne cm., so that the equation of motion of the inner cylinder P is

$$I\ddot{\theta}+R\dot{\theta}+E\theta=k(\Theta-\theta) \qquad (1)$$

where $I\ddot{\theta}$ is the inertial resistance, and $R\dot{\theta}$ and $E\theta$ are the viscous and elastic resistance respectively of the visco-elastic body existing among the two cylinders, and $k(\Theta-\theta)$ is the external torque imposed on the inner cylinder. T. Kuyama[3] suggested a method for studying

(1) Read before the 4 th annual meeting of the Chemical Society of Japan on Apr. 8, 1951.

(2) Details of the method will appear in *J. Chem. Soc. Japan*, **72**, 759(1951).

(3) T. Kuyama, *Kagaku (Science)*, **16**, 149 (1946).

the visco-elastic effect from the graphical analysis of the stress-strain hysteresis loop.

The author, in the present study, has used a modified scheme. (1) is rewritten as

$$\ddot{\theta}+2\varepsilon\dot{\theta}+n_e^2\theta=L\sin\omega t \qquad (1')$$

$$2\varepsilon\equiv R/I,\ n_e^2\equiv(k+E)/I,\ L\equiv k\Theta_0/I \qquad (1'a)$$

The stationary solution of (1') is

$$\theta=A\sin(\omega t-\phi)\equiv m\Theta_0\sin(\omega t-\phi) \qquad (2)$$

where $$\tan\phi=2\varepsilon\omega/(n_e^2-\omega^2), \qquad (2a)$$

and

$$m\equiv A/\Theta_0=\frac{k}{I\sqrt{(n_e^2-\omega^2)^2+4\varepsilon^2\omega^2}} \qquad (2b)$$

As is plain from (2a) and (2b), it is possible to calculate R and E from the observed phase difference ϕ and the amplitude ratio m at the stationary state of the forced oscillation, by using the next relations

$$\left.\begin{aligned} R&=\frac{kT\sin\phi}{2\pi m}\\ E&=k\left(\frac{\cos\phi}{m}-1\right)+\frac{4\pi^2 I}{T^2}\end{aligned}\right\} \qquad (3)$$

where T is the period ($\omega=2\pi\nu=2\pi/T$).

If R and E are determined, viscosity η poises and rigidity G dyne/cm.^{2} of the substance are known from the following formulas[4][5]:

$$\left.\begin{aligned}\eta&=\frac{R}{4\pi l}\left(\frac{1}{r_1^2}-\frac{1}{r_2^2}\right)\equiv K_0 R\\ G&=\frac{E}{4\pi l}\left(\frac{1}{r_1^2}-\frac{1}{r_2^2}\right)\equiv K_0 E\end{aligned}\right\} \qquad (4)$$

where l, r_1, and r_2 are the lateral length of the immersed portion of the inner cylinder, radius of the inner and the outer cylinder respectively.

In the present measurement the experimental condition is as follows.

$I=8.76\times10^3$ g. cm^2.;

$k=1.12\times10^5$ dyne cm. (piano wire of 1 mm. diameter, 72 cm. length);

$r_1=2.50$ cm.; $r_2=3.70$ cm.; l, about 16 cm. in all cases;

$\Theta_0=8°45'$ (0.153 radians), so that A is less than that;

T, 3 min. to 20 min.; temp., $80\sim110°\pm0.1°$.

In the case of large T as in the present, the term $4\pi^2I/T^2$ in (3) can be omitted. Temperature control was done by the oil bath thermostat regulated in the ordinary manner. Thermal uniformity in the cylinder was so slowly reached for the large dimensions of the vessel that it was necessary to wait about two hours or more before measurement was begun. The sinusoidal motion was supplied by the mechanism of the crank-shaft principle. Deflections Θ and θ were read by the method of lamp-and-scale by means of the two small galvanometer mirrors attached to the upper disk and the lower cylinder. The phase angle ϕ is given by

$$\phi=\frac{\tau}{T}\times2\pi \qquad \text{radians}$$

where τ sec. is the measured time interval between the instant when O passes $\Theta=0$ and the instant when P passes $\theta=0$; $\Theta=0$ and $\theta=0$ corresponding to the middle point of the rotational oscillation. The torsion constant k was determined from the period T_0 of the free oscillation with a weight of the known moment of inertia I_0 by

$$k=4\pi^2I_0/T_0^2.$$

It should of course be kept in mind that k changes with the length of the wire.

Coal Tar Pitches.—Pitches from coal tar of ordinary high temperature carbonization were subjected to test. Their origin and the conventional softening temperature are tabulated below (Table 1).

Table 1

Abbreviation	Origin	So-called softening point, °C.
Tar pitch N	Nisshin Kagaku Co.	80
O	Osaka Gas Co.	—
H	Hirohata Iron-Works	79
Y	Yahata Iron-Works	65

Results and Discussions

Frequency Dependence of η and G.—Figs. 2 and 3 show frequency dependence of viscosity η and rigidity G at various temperatures. As is read from the figures, no appreciable frequency effect upon η was observed. Elastic nature is very slight in this frequency range. G cannot be detected at higher temperatures, and becomes appreciable first at lower temperatures. Rheological property of tar pitch so is simply Newtonian for such comparatively

(4) E. Hatschek, "The Viscosity of Liquids," G. Bell and Sons, Ltd., London, 1928.
(5) Th. Schwedoff, *J. de Phys.* [2] **8**, 341 (1889).

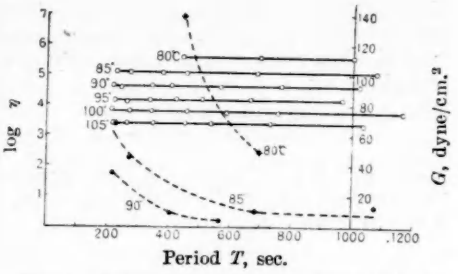

Fig. 2.—Frequency dependence of η and G of tar pitch H: —— indicates the frequency dependence of η and - - - -, that of G,

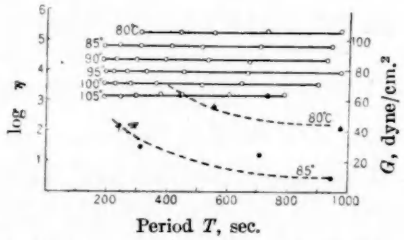

Fig. 3.—Frequency dependence of η and G of tar pitch Y: —— indicates the frequency dependence of η and - - - -, that of G.

slow observation as in the present case. It is supposed that the time of mechanical relaxation is less or far less than several minutes in these temperatures, so that the mechanisms of elastic strain in the internal structure, if they exist, will decay into the mechanisms of viscous flow in our experimental condition of a long period. Elastic effect may on the other hand become remarkable if they are treated in the range of far larger frequency, *e. g.*, audiofrequency range[6] for which our experimental device is not available.

From the rheological point of view, frequency dependence of the visco-elastic properties as has appeared in Figs. 2 and 3 will be interpreted as follows. Our whole experimental procedure and scheme of analysing the observed values depend on the assumption that the rheological properties of the material can be simply symbolized by the Voigt model (viscosity and elasticity in parallel) as is schematized in Fig. 4 b. If the material is truly of Voigt type in the rheological behavior, R and E, or η and G will appear as constant. But, on the other hand, if it is intrinsically of Maxwell type as in Fig. 4 a, the Voigt scheme analysis

(6) See, for example, J. D. Ferry *et al.*, *J. App Phys.*, **20**, 144 (1949).

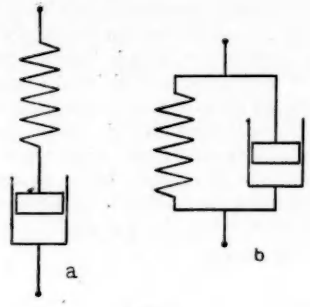

Fig. 4.

of it should lead to η and G variant with frequency or amplitude. Assume, now, that tar pitch is a simple Maxwellian body as the first approximation, then the Voigt type analysis of its rheological behavior should bring about the result that viscosity remains constant regardless of period, and that elasticity vanishes with the increase of period. This situation coincides with our observed data.

From the above-stated, it will be admitted that tar pithch is a Maxwellian body (viscosity and elasticity in series, *cf.* Fig. 4 a) with respect to the rheological behavior.

Temperature Dependence of Viscosity.—As has been stated above, viscosity is constant in our frequency range. An arithmetical mean of viscosity data at the same temperature was taken as viscosity at the temperature, and was plotted against $1/T$ °K. in Fig. 5. η falls to

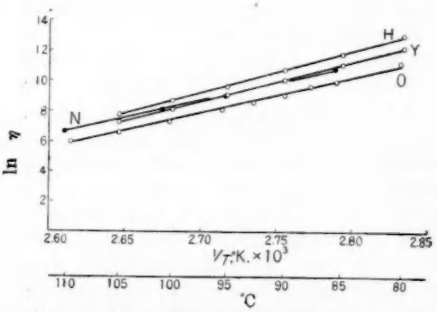

Fig. 5.—Temperature dependence of η: $\eta = Ae^{B/T}$.

about 1/3 by the increase of 5° of temperature, the sensitivity of η to temperature being remarkable compared with the ordinary low molecular weight liquids.

The author has used the Andrade formula

$$\eta = Ae^{B/T} \qquad (5)$$

to express the temperature sensitivity of η, and determined A and B by the method of least squares. Results are given in Table 2, and the values for some other materials calculated from other authors' data are shown in Table 3[7] for the sake of comparison. A high value of B indicates that the substance is highly associated, a large amount of energy being necessary to bring about the dissociation. To what is the large negative value of $\log A$ attributed?

Table 2

Material	$-\log A$	$B\times10^{-3}$
Pitch N	23.4	23.2
O	23.7	23.2
H	27.9	27.2
Y	25.5	25.1

Table 3[7]

Material	Temperature range, °C.	$-\log A$	$B\times10^{-3}$
Glass below T_g(1)	400~500	23.2	63.2
Glass below T_g(2)	400~500	26.0	65.7
Glass above T_f	700~1400	5.6	28.6
Undercooled glucose	22~40	62.4	51.8
Undercooled glucose	110~145	11.7	11.9
Rosin	25~60	44.1	38.1
Abietic acid	20~50	42.9	37
Pitch	20~40	35.6	30.9
Asphalt A	15~50	22.3	20
Asphalt A	80~130	10.8	11
Asphalt D	15~50	22.6	20
Asphalt D	80~130	11.0	11
Mercury	−20~300	2.23	0.29
Toluene	0~100	3.76	1.04
Water	0~20	5.44	2.32
Water	50~100	4.36	1.56

According to the theory of flow by the method of transition state,[8] viscosity η is formulated as

$$\eta=\frac{h}{\lambda_1\lambda_2\lambda_3}e^{\Delta F^*/RT} \qquad (6)$$

where h is Planck's constant, λ are dimensions of the unit of flow, and ΔF^* is the free energy of activation which is necessary for the unit of flow to be activated up to the transition state from its initial state. Further, since ΔF^* may be replaced by

$$\Delta F^*=\Delta H^*-T\Delta S^*,$$

where ΔH^* and ΔS^* mean the heat of activation and the entropy of activation respectively, it is seen that

$$\eta=\left(\frac{h}{\lambda_1\lambda_2\lambda_3}e^{-\Delta S^*/R}\right)e^{\Delta H^*/RT}. \qquad (7)$$

From the comparison of (7) with (5) it comes that

$$A=\frac{h}{\lambda_1\lambda_2\lambda_3}e^{-\Delta S^*/R},\quad B=\Delta H^*/R. \qquad (8)$$

It is therefore, from (8) and Table 2, that

$$\Delta H^*\doteqdot 50 \text{ kcal.}$$

From the rate-process view-point, the high value of ΔH^* is to be attributed to the fact that, in addition to the normal work required to make a hole, it is necessary for the secondary bonds, whereby a pitch particle is attached to the surrounding particles, to be broken before the activated state for flow can be attained. There is consequently what might be termed as a "structure activation energy", in addition to the normal activation energy, for the flow of such associated fluids as pitch.

The estimation of ΔS^*, on the other hand, will meet with some complexity for the sake of the co-existing volume factor $\lambda_1\lambda_2\lambda_3$. The large negative value of $\log A$ in Table 2 nevertheless postulates that ΔS^* has a large positive value, which is about 85 E.U. if λ is assumed to be 100 Å., while the entropy of activation ΔS^* is usually negative in the case of flow of the ordinary non-associated substances. If, as suggested above, the unit of flow even in associated fluids is a single particle and the formation of the activated state involves the breaking of a number of secondary bonds, it is evident that the entropy of the activated state will be appreciably greater than that of the initial state. In other words, the entropy of activation for flow ΔS^* should be relatively large and positive in agreement with our experimental fact.[9]

At the higher temperature, there is no secondary bond that has to be broken before flow

(7) The data for constructing this table are borrowed from the following authors. Glass: F. B. Hodgdon and D. A. Stuart, *J. Appl. Phys.*, **21**, 1160 (1950). Glucose: G. S. Parks *et al.*, *Physics*, **5**, 193 (1934). Rosin, abietic acid, and pitch: E. C. Bingham and R. A. Stephens, *Physics*, **5**, 217 (1934). Asphalts: C. U. Pittman and R. N. Traxler, *Physics*, **5**, 221 (1934). Mercury, toluene, and water: "Smithsonian Physical Tables."

(8) S. Glasstone, K. J. Laidler and H. Eyring, "The Theory of Rate Processes," McGraw-Hill Book Co., Inc., New York, 1941.

(9) Another example that the high value of ΔH^* is compensated by the large positive value of ΔS^* is illustrated in the kinetics of the protein denaturation (cf. note (8)).

can occur, and hence the activation energy ΔH^* will decrease and the entropy term $\log A$ will take a smaller negative value. See the case of glass in Table 3, where T_g is an abbreviation of the German "Temperatur des Glaszustandes" and T_f means "Temperatur des Fadenziehens."

The above-stated conception of the internal structure of tar pitch derived from the analysis of its viscosity in the softening range seems to be reconciled with the theory of the internal structure of coal, in which such nuclei as ash or graphite are considered to be strongly solvated with bitumen. It is probable that in the solid tar pitch, as in coal, the so-called "free carbon" or graphite-like particles are solvated with the bituminous substance, and that such associated structure is conserved even at the softening temperature.

Summary

(1) Visco-elastic properties of tar pitches in the softening range were measured by a dynamic method covering 3~20 minutes of period.

(2) No frequency dependence of viscosity was observed in this range of period.

(3) Elastic effect was slight in this range of period. Its frequency dependence was appreciable.

(4) Tar pitch is a simple Maxwellian body rheologically above the softening point.

(5) Temperature dependence of viscosity was studied along the rate-process theory, and it was supposed that tar pitch has a highly associated or solvated structure, consistent with the present theory of the internal structure of coal.

The author wishes to express his gratitude to Professor J. Sameshima and Dr. H. Akamatu for their encouragement. He is also indebted to several organizations (Table 1), for samples. These experiments were largely supported by the Scientific Reseerch Encouragement Grant defrayed from the Ministry of Education, to which the author's thanks are due.

Department of Chemistry, Faculty of Science, the University of Tokyo, Tokyo

Thermal Diffusion Coefficient and its Relation to Ordinary Diffusion Coefficient of Solutions

By Kozo HIROTA and Isao MIYASHITA

(Received May 30, 1951)

Though a number of theoretical formulas regarding thermal diffusion effect of solutions or the Ludwing-Soret effect have been proposed from the standpoint of kinetic theory or thermodynamics, it seems to us that they are not accepted generally. This is the reason why one of the present writers (K. H.)[1] derived a formula, adopting the cage model to the solution and applying the activated state method to the system. According to the formula, the Soret coefficient and thermal diffusion coefficient of the solute molecules whose molecular weight is 100 were calculated to be 1×10^{-3} and 6×10^{-3} respectively at 50°, if two kilocalories were assigned to the energy of activation for crossing the cage-barrier. They fall in the range of usual experimental values of aqueous electrolyte solutions (HCl, KCl, NH_4Cl, H_2SO_4, etc.). However, this successful result contained some ambiguity due not only to the absence of reliable data on the energy of activation and other quantities of such systems, but also to the inevitable occurrence of thermal diffusion potential. Because, in the case of electrolyte solutions each ion cannot behave as a perfectly independent particle hindered by their mutual electrical action as shown experimentally.[2],[3]

Considering the matter, it is desirable to check the theory with some experimental data of non-electrolyte solutions, though they are

(1) K. Hirota, and O. Kimura, This Bulletin, **18**, 111 (1943); *cf.*, *Chem. Abst.*, **41**, 436 (1947).

(2) K. Hirota, This Bulletin, **16**, 475 (1941).

(3) G. Guthrie, J. N. Wilson and V. Schomaker, *J. Chem. Phys.*, **17**, 310 (1949).

very few in number. However, as there appeared some reliable measurement which can meet the requirement, the present research was begun again with reference to ordinary diffusion, transforming the theoretical result into the formulas which can easily be checked experimentally.

Theoretical Formulas

a) Thermal Diffusion Coefficient.— According to the transition state method, the rate of jump of a solute molecule from a cage to a neighboring one can be given by the expression,[4]

$$\vec{\Re} = \frac{kT}{h} \exp\left(-\frac{\Delta H^*}{RT} + \frac{\Delta S^*}{R}\right), \quad \cdots(1)$$

where k, h, and R denote the Boltzmann, Planck, and gas constants, respectively, while ΔH^* and ΔS^* denote enthalpy of activation and entropy of activation, respectively. The transmission factor was regarded to be unity as is done usually.

Now the application of the above formula, which was deduced under the condition when the whole system is kept at constant temperature, is extended to the system in which thermal gradient exists stationarily. (The relation of the energy against distance x is shown schematically in Fig. 1.) Therefore, taking the

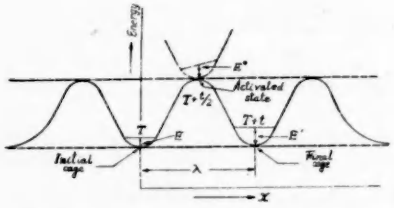

Fig. 1.—Schematic model of the cage-energy relation: Dotted lines at the activated state denotes that they are perpendicular to the plane of the paper.

temperatures of the equilibrium positions of initial and final cages (T and $T+t$) into consideration, the rate of translation from the initial cage to the final can approximately be given by

$$\vec{\Re} = \frac{k\left(T+\frac{1}{2}t\right)}{h} \exp\left(-\frac{\Delta H^*}{R\left(T+\frac{1}{4}t\right)} + \frac{\Delta S^*}{R}\right), \quad (2)$$

because T of the exponential term can be replaced by the mean of those of T and $T+\frac{1}{2}t$, the temperature of the activated state, while kT/h in Eq. (1) is to be replaced by $k(T+\frac{1}{2}t)/h$, as it was derived from the partition function over the coordinate of the reaction path at the activated state.

As the rate formula to the opposite direction $\overleftarrow{\Re}$ will be similarly given by

$$\overleftarrow{\Re} = \frac{k\left(T+\frac{1}{2}t\right)}{h} \exp\left(-\frac{\Delta H^*}{R\left(T+\frac{3}{4}t\right)} + \frac{\Delta S^*}{R}\right), \quad (2')$$

the mean distances moved per second by the solute molecule equal to or against the temperature gradient will be $\vec{\Re}$ or $\overleftarrow{\Re}$ multiplied by the distance of the neighboring cages, λ, respectively.

The flow velocity of the solute molecules, whose concentration c is so small that the flow of solvent is negligible, will be given by

$$v = c\lambda(\vec{\Re} - \overleftarrow{\Re}), \quad \cdots\cdots(3)$$

if $\mathrm{d}\Delta H^*/\mathrm{d}T$ and $\mathrm{d}\Delta S^*/\mathrm{d}T$ are assumed to be the quantities considered in the higher order of approximation.

Phenomenologically thermal diffusion coefficient D' in solution is defined by the proportional constant in the expression of diffusion flow v, which is produced by the temperature gradient $\mathrm{d}T/\mathrm{d}x$.

$$v = -D'c(\mathrm{d}T/\mathrm{d}x). \quad \cdots\cdots(4)$$

Thus from Eqs. (3) and (4),

$$D' = -(\mathrm{d}x/\mathrm{d}T) \cdot (\vec{\Re} - \overleftarrow{\Re}). \quad \cdots\cdots(5)$$

Considering that

$$\exp\frac{-\Delta H^*}{R\left(T+\frac{1}{4}t\right)} - \exp\frac{-\Delta H^*}{R\left(T+\frac{3}{4}t\right)} \simeq \frac{-t\Delta H^*}{2RT} \exp\frac{-\Delta H^*}{RT} \quad \cdots\cdots(6)$$

and

$$\frac{\mathrm{d}T}{\mathrm{d}x} = \frac{t}{\lambda}, \quad \cdots\cdots(7)$$

we obtain from Eqs. (2), (2') and (5)

$$D' = \frac{\lambda^2 k}{2h} \frac{\Delta H^*}{RT} \exp\left(\frac{-\Delta H^*}{RT} + \frac{\Delta S^*}{R}\right). \quad (8)$$

(4) Glasstone, Laidler and Eyring, "Theory of Rate Processes," 1941, p. 522.

b) Relations between Thermal Diffusion and Ordinary Diffusion.—The ordinary diffusion coefficient D was derived theoretically by Eyring and others as follows:[5]

$$D=\frac{\lambda^2 kT}{h}\exp\left(\frac{-\Delta H^*}{RT}+\frac{\Delta S^*}{R}\right). \quad \ldots(9)$$

Differentiating Eq. (9) with respect to T, we obtain easily from Eqs. (8) and (9)

$$D'=\frac{1}{2}\left(\frac{\mathrm{d}D}{\mathrm{d}T}-\frac{D}{T}\right). \quad \ldots\ldots\ldots(10)$$

Soret coefficient defined by D'/D, therefore, can be expressed by

$$\text{Soret Coef.}=\frac{1}{2}(\mathrm{d}\ln D/\mathrm{d}T-1/T). \quad (11)$$

For convenience sake of discussion in the last article, the corresponding formulas of Wirtz,[6] who also used the cage model and applied the method of elementary kinetic theory, will be cited, *i. e.*,

$$D'=\mathrm{d}D/\mathrm{d}T, \quad \ldots\ldots\ldots\ldots\ldots(12)$$

$$\text{Soret Coef.}=\mathrm{d}\ln D/\mathrm{d}T. \quad \ldots\ldots\ldots(13)$$

Experimental Method of Evaluating ΔH^*, ΔS^*, etc.

In order to determine the theoretical D', it is necessary to evaluate λ, ΔH^* and ΔS^* in Eq. (8). The most direct way to meet the requirement is to make use of the data of ordinary diffusion, because the temperature dependence of thermal diffusion is not studied yet in details. But with the exception of mannitol, there is no system whose measurement on D as well as D' has been carried out over so wide a temperature range that ΔH^* can be determined by plotting in (D/T) against $1/T$ to make use of Eq. (9).

The second way of estimating is afforded by viscosity η. According to the transition state theory, it is given by the formula

$$\frac{1}{\eta}=\frac{\lambda_x\lambda_y\lambda^2}{\lambda_z h}\exp\left(\frac{-\Delta H^*}{RT}+\frac{\Delta S^*}{R}\right), \quad (14)$$

where λ_x is the distance between the two adjacent layers of molecules (sliding each other), while λ_y and λ_z are perpendicular distances between the neighboring positions in the plane perpendicular to the shearing motion. By a number of researches viscosity has been measured over such a wide and various temperature range that ΔH^* can be determined easily, but to our inconvenience it is difficult to know the required term $\exp(\Delta S^*/R)$. Because, even if the factor independent from temperature in Eq. (14) is determined experimentally, the factors λ_x, λ_y and λ_z and therefore their product $\lambda_x\lambda_y\lambda_z^{-1}$ are hard to be estimated from the other source of data.

The third method of estimation is based on the dielectric relaxation. According to Eyring, the so-called relaxation time τ_0 is given by

$$\frac{1}{\tau_0}=\left(\frac{kT}{h}\right)\exp\left(\frac{-\Delta H^*}{RT}+\frac{\Delta S^*}{R}\right). \quad (15)$$

Strictly speaking, these remains an important question if ΔH^* and ΔS^* evaluated by these three methods can be identified to those of thermal diffusion, because the mechanisms of these rate processes are not the same. Actually it was shown experimentally by the studies on the relation between τ_0 and η.[9]

However, as it seems that ΔH^* and ΔS^* can be estimated easily by the third method, the result obtained by the method will be used in the next paragraph for the check of Eq. (8). This attempt may, however, be admitted as the first approximation; because the solute molecule which rotates in the alternating electric field seems to produce as much disturbance on solvent molecules as that when the former jumps over the cage barrier, considering the situation that it is forced to rotate making the part of dipole which does not locate at the molecular center in the present ases.

Comparison of the Theoretical Diffusion Coefficient with the Observed

Recently, Higasi and Nukasawa[10] determined ΔH^* and ΔS^* of the solutions of cane sugar and ethyl alcohol by measuring their complex dielectric constants at 0–30°, using the electric wave of 10.45 cm. in wave length and arranging the data by the Cole-Cole method. Their results are shown in the second and third columns of Table 1. For the sake of reference, the values of ΔH^* obtained from

(5) G., L., and E., *ibid.*, p. 524.
(6) K. Wirtz, *Naturwiss.*, **27**, 369 (1939); *Ann. Phys.*, **36**, 295 (1939).
(7) G. L. E., *ibid.*, p. 483.
(8) G. L. E., *ibid.*, p. 548.
(9) A. Bondi. *J. Chem. Phys.*, **14**, 541 (1946); Kauzmann, *Rev. Mod. Phys.*, **14**, 12 (1942); C. P. Smyth, *et al.*, *J. Am. Chem. Soc.*, **72**, 3447 (1950); **70**, 4102 (1948).
(10) K. Higasi and K. Nukasawa, unpublished result. Difference of the data between the preliminary report (*J. Chem. Phys.* **18**, 561 (1950)) and the present was brought about by the change of evaluation of their data.

viscosity data are shown in the fourth column of the table. They coincide with those obtained from relaxation time satisfactorily.

Table 1

Experimental Check of Eq. (8)

System	$\Delta H^{\neq}$ Calc. from τ_0, kcal.	$\Delta S^{\neq}$ Calc. from τ_0, E. U.	$\Delta H^{\neq}$ Calc. from η, kcal.	D' Calc., $\times 10^5$	D' Obs., $\times 10^5$
Ethyl alcohol (20wt%)-water	6.0	10	5.3	8	1.5 (40°C.)*
Cane sugar (10wt%)-water	5.4	9.7	4.3	7	0.34 (30°C.)**

* P. F. van Velden, H. G. P. van der Voort and C. J. Gorter, *Physica*, **12**, 151 (1946).

** J. van Dranen and F. Bergsma, *Physica*, **13**, 558 (1947).

On the other hand, thermal diffusion coefficients of ethyl alcohol and cane sugar in aqueous solution are calculated according to Eq. (8), by the use of 1.44 Å. (0°) —1.47 Å. (45°) as the distance between the two neighboring cages.[11] They are given in the fifth column of Table 1. It will be seen that the calculated value of ethyl alcohol (8×10^{-8}) is of the same order of magnitude as the experimental (1.5×10^{-8}) at 40°. However, the calculated value of cane sugar (7×10^{-8}) is larger at least by twenty times than the experimental one (3.4×10^{-9}).

A possible cause of such disagreement will be due, besides the neglect of transmission factor, not only to the use of the molecular diameter of water as λ, but also to the assumptions made in the theory, *i. e.*, substitution of ΔH^{*} and ΔS^{*} determined from dielectric relaxation time for those of thermal diffusion. In fact, though the hindrance during diople rotation, which is brought about by electric force, may be large, the energy required seems to be less than that of making a sufficiently large hole in the neighboring cage crossing the potential barrier of the cage, while the entropy required will be also different in both phenomena. Considering the situation, the above agreement can be said to be satisfactory.

As the alternative cause of disagreement, the mechanism similar to that of ordinary diffusion must be mentioned; *i. e.*, according to Eyring the diffusion of large solute molecules is realized by the successive movement of small solvent molecules around the solute molecule. It will be shown by the discussion in the next paragraph, which is the more plausible cause of the two.

Relation of Ordinary Diffusion Coefficients with Thermal Diffusion Coefficients

First, aqueous solutions of mannitol (0.01 mole/liter) and cane sugar (10 wt%) will be discussed as the example of the non-electrolyte solution, in order to check Eq. (10). Regarding the solution of mannitol, the Soret coefficient was measured carefully over the wide concentration range down to infinite dilution, while the diffusion coefficient was determined over the temperature ranges between 0° and 60°.[12] Thus the enthalpy of activation obtained by plotting $\ln(D/T)$ is 4.2 kcal. as described in Table 2 together with dD/dT at 35°. As the observed thermal diffusion coefficient is 0.6×10^{-8} at 35°, the one calculated according to Eq. (10) is given as 8×10^{-8}, the calculated is larger by twelve times than the observed. A similar result was obtained regarding to the cane sugar as is shown in the second system of Table 2.

Table 2

Experimental Check of Eq. (10)

System	Mean temp., °C.	D, $\times10^5$	dD/dT, $\times10^7$	$\Delta H^{\neq}$, kcal.
Mannitol	35	0.81	1.8	4.2
Cane sugar	15	0.36	1.06	4.8
Hydrogen chloride	50	5.8	8.1	—
$AgNO_3$-KNO_3	400	4.3	0.96**	—

System	D' (calc.)	D' (obs.)
Mannitol	8×10^{-8}	0.6×10^{-8} (35°)
Cane sugar	4.7×10^{-8}	0.3×10^{-8} (30°)
Hydrogen chloride	3.1×10^{-7}	1.7×10^{-7} (50°)*
$AgNO_3$-KNO_3	0.18×10^{-7}	1.5×10^{-7} (400°)

* Calculated from Soret coefficient and diffusion coefficient.

** Landolt-Börnstein, "Phys.-Chem. Tabellen," II Erg. Band, p. 199.

It is noteworthy that the above disagreement is the same in tendency as was found in the check of Eq. (8) regarding cane sugar, the molecule of which is large. Therefore, the second mechanism suggested in the last paragraph seems to be held to such systems, but it must be abandoned because the effect ascribable to the movement of small solvent

(11) These values were determined by the self-diffusion coefficient. Eyring, *J. Chem. Phys.*, **4**, 283 (1936).

(12) Landolt-Bornstein, "Phys. Chem. Tabellen," II Erg. Band, p. 190.

molecules occurs in the case of an ordinary diffusion as well as in the case of a thermal diffusion, giving no net effect to the check of Eq. (10).

Second, hydrochloric acid will be utilized for our purpose, as the example of electrolyte solution. As shown in Table 2, the measured thermal diffusion coefficient of 1 N HCl is given to be 1.7×10^{-7} at 50°, while the calculated is 3.1×10^{-7} by the use of dD/dT (8.1×10^{-7}), and D extrapolated at 50° (5.8×10^{-5}).[1] Such an unexpectedly good theoretical result seems to be due to the cancellation of the effect of a thermal diffusion potential by that of an ordinary diffusion potential, because both effects are included in the observed values. However, the above good coincidence could not be obtained in the last system of Table 2, *i. e.*, molten $AgNO_3$($AgNO_3$, 3%); the observed value (1.5×10^{-7}) is about seven times larger than that of the calculated.[13] The result obtained here may not be strange, considering that the system consists entirely of ions and electrical interaction is very large.

In concluding our discussion, it will be added that the calculated value by the use of Eq. (12) will become larger at least by two times than the above in every case, making the discrepancy increase by the same factor. Secondly it must be mentioned that Eq. (11) derivable from Eq. (10) was proposed already by Wereide[14] from the standpoint of the elementary kinetic theory of solution, taking the motion of solvent molecules into account. However, according to this theory, the formula can be applied only when the size of a solute molecule is much larger than that of solvent molecules, while Soret coefficient is to be negligibly small when the size of both molecules is of the same order of magnitude. The conclusion cannot be supported by the experimental result of Hirota and Kimura[15]; *e. g.*, they confirmed by means of a Clusius-Dickel's thermal diffusion apparatus that though the separation of some sols (gelatine and hydrogen sulfide) was larger than that of usual electrolyte solutions, the separation of other sol (ferric hydroxide) was not observed definitely. Therefore, it is not wonderful that Wereide could not confirm his own formula experimentally regarding electrolyte solutions. According to the present theory, thermal diffusion coefficient will be given by Eq. (11) in the system whose molecule is not extremely large if compared with solvent molecules, while in the systems of large solute molecules it may become smaller than the value calculated by Eq. (11).

Summary

Theoretical formulas of thermal diffusion coefficient D' and its relation to ordinary diffusion coefficient D have been derived by applying the activated state method to the solution in which stationary thermal gradient exists. Regarding the solution of small solute molecules, whether it is electrolytic or non-electrolytic, the agreement with experimental result is good, while, regarding the solution of large solute molecule or molten salt, the discreparcy amounts to one order of magnitude.

Research Institute of Applied Electricity
Hokkaido University, Sapporo

(13) K. Hirota and others, *J. Chem. Soc. Japan*, **64**, 811 (1943).
(14) T. Wereide, *Ann. de physique*, **2**, 55 (1914).
(15) O. Kimura and K. Hirota, *J. Chem. Soc. Japan*, **65**, 113 (1944).

Studies on Monomolecular Films. IV. Stabilization of Monoparticle Films of Nonpolar Substances by Stearic Acid

By Ryôhei MATUURA

(Received June 2, 1951)

Introduction

In order to spread on the surface of water and form a stable film a substance must have a polar-nonpolar structure, but we may be much interested in a surface film of a nonpolar substance which, if formed, would give a knowledge concerning the size and the shape of its particle on the surface of water. It is certainly true that a nonpolar substance is not capable of forming a stable film on water by itself, but it can be made to spread by mixing with a polar substance, such as fatty acids, as has been demonstrated by the work of Zisman.[1] The present author showed in the preceding paper[2] the possibility of obtaining the stable surface films of a nonpolar substance according to this principle when it was mixed with a film-forming substance such as stearic acid, and there it was suggested that the structure of the surface film of various nonpolar substances or other nonspreadable matters might be studied by means of such mixed films. Stearic acid could be considered as a stabilizer for the surface film formation of nonspreadable substances. In the present work it was attempted to prepare the surface films of some nonpolar substances by mixing with stearic acid and to discuss the structure of the particles in the films thus formed on water as well as the mechanism of stabilizing action of stearic acid, taking into account of the results of measurements of pressure~area and area~composition characteristics.

Experimental

Apparatus.— The surface pressure of the film was measured by the simple method of Sasaki based on the principle of Wilhelmy's surface tension measurement. A glass slide 2.59 cm. wide and 0.151 cm. thick was used as a pendant plate, which enabled us to measure the surface pressure down to 0.1 dyne/cm.

Material.— Nonpolar substances used in this experiment were fully purified by the repeated recrystallization or the vacuum distillation, except for the high-molecular substances such as raw rubber and polystyrene which were used without particular purification. As a fatty acid to be mixed with nonpolar substances, stearic acid, purified by recrystallization, was used. A nonpolar substance and stearic acid were mixed in varying proportions and the mixture was spread from benzene solution on the surface of $N/100$ hydrochloric acid by means of an automatic microvolume pipette.[3]

Experimental Results.

As an example, a pressure~area diagram of mixed films of paraffin hydrocarbon (m. p. *ca.* 53°) and stearic acid on the surface of $N/100$ hydrochloric acid is shown in Fig. 1.

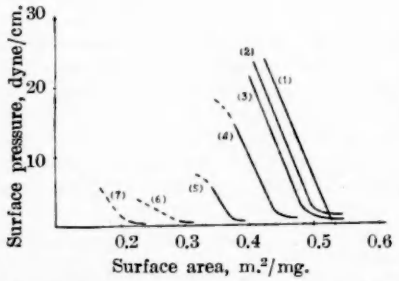

Fig. 1.—Pressure~area relations of mixed films of paraffin (m. p. 53°) and stearic acid on $N/100$ HCl at 22°. Stearic acid content in mixture: (1) 100%; (2) 95%; (3) 91%; (4) 77%; (5) 50%; (6) 33%; (7) 9%.

Paraffin was hardly capable of forming a surface film by itself on $N/100$ hydrochloric acid, but when mixed with stearic acid it could be made to spread and form a mixed film. The mixed film thus obtained was, however, very unstable and collapsed easily on compression when the acid content was low. It became more and more stable as the acid content increased. The dotted lines in Fig. 1 show the

(1) W. A. Zisman, *J. Chem. Phys.*, **9**, 534 (1941).
(2) R. Matuura, *Memoirs of the Faculty of Science, Kyushu University, Ser. C*, Vol. 1, 69 (1949).
(3) T. Sasaki, *J. Chem. Soc. Japan*, **62**, 796 (1941); R. Matuura and I. Hayasi, *Memoirs of the Faculty of Science, Kyushu University, Ser. C*, Vol. 1, 31 (1948).

pressure~area curves obtained temporarily by rapid compression. When the zero-compression areas in Fig. 1 are plotted against the composition of the mixture, a curve as shown in Fig. 2 is obtained. When the content of stearic acid in the mixture is small, the area of the mixed films cannot be determined exactly because of their instability, while when the content exceeds 50% the films are stable enough to allow the accurate determination of area. In this region the area~composition curve proves to be linear, suggesting that paraffin hydrocarbon and stearic acid form the mixed surface films without special interaction between two constituents, at least in an uncompressed state. Such a consideration is analogous to the case of three-dimensions where

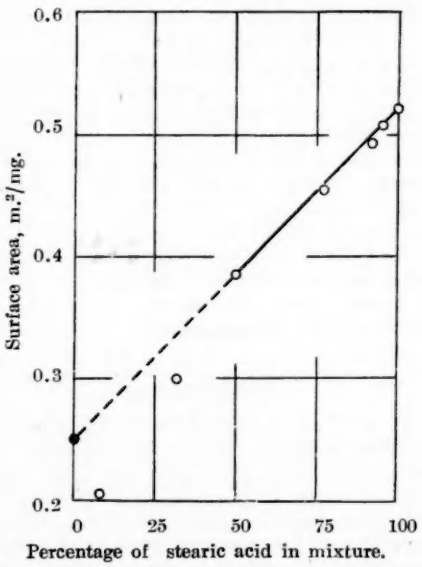

Fig. 2.—Area-composition relation of mixed films of paraffin and stearic acid on $N/100$ HCl at 22°.

the specific volume~composition curve is linear for ideal solutions. Thus the limiting area, obtained when the area-composition curve is extrapolated to the zero acid content, is reasonably assumed to be the surface area occupied alone by paraffin film. The surface area of paraffin film thus obtained on $N/100$ HCl at 22° is 0.25 m.²/mg. Assuming the surface particle of paraffin to be spherical and one layer thick, and the density same as in bulk, its radius is calculated to be 40 Å. The size of the surface particle of another paraffin hydrocarbon (m. p. *ca.* 47°) is somewhat smaller, its radius being about 30 Å. By a similar treatment we further calculate the dimension of particles of some other nonpolar substances in surface films stabilized by stearic acid on $N/100$ hydrochloric acid. The results are shown in Table 1. Some of them form thick films by themselves, but the films are often so unstable that they readily collapse under low lateral compression without the aid of stearic acid.

Table 1

The Size of Particles in Surface Film on $N/100$ HCl

Substance	Film area, m.²/mg.	Radius of particle, Å.
Paraffin hydrocarbon (m. p. 53°)	0.25	40
Paraffin hydrocarbon (m. p. 47°)	0.32	30
Anthracene	0.11	55
Phenanthrene	0.10	71
Chlornaphthalene (m. p. 100–110°)	0.03	200
Triphenylmethane	0.01	—
Polystyrene	0.11	68
Raw rubber	0.02	370

Discussion

If a nonpolar substance is dropped alone as a benzene solution on the surface of water, it may spread temporarily due to the spreading force of benzene, but no surface film is left behind after the solvent evaporates up. We get merely macroscopic crystallines of the substance floating on water. On the other hand, high-molecular substances such as polystyrene or raw rubber form the thick films on water, but they are again too unstable to give the precise knowledge concerning their structure. However, when mixed with stearic acid, they form a fairly stable surface film on water in the case where the acid content is large, thus enabling us to discuss the structure of these films. Here stearic acid seems to act as a stabilizer for the surface films of nonpolar substances.

It is, however, seen in Table 1 that the surface films of nonpolar substances thus obtained in this experiment are not monomolecular but are much thicker. Even in the case of paraffin hydrocarbon where the surface film occupies rather larger area, the molecules of hydrocarbon cannot be considered as arranging themselves in monomolecular layer. Thus, with paraffin of melting point 47° which may well be considered as consisting largely of *n*-tricosane, the area per molecule of the paraffin in the film is calculated to be 15.5 Å.² with the

assumption that it can form a monomolecular layer on water by the aid of stearic acid. This value is still too small as the cross-sectional area of paraffin chain, therefore, it is evident that the above assumption cannot be adopted. Paraffin, and also all the other nonpolar substances studied in this experiment form polymolecular films, as pointed out by Harkins *et al.*[4] and Aron and Frenkel.[5] But the present author should like to call them "monoparticle films" or simply micellar films consisting of particles of aggregated nonpolar molecules instead of polymolecular films. The particles are held and interlocked with the molecules of stearic acid, forming together a stable surface film on water. The size of the particle in the surface film is given for each nonpolar substance studied as shown in Table 1. This particle may be taken as a comparatively stable unit appearing in the process of aggromeration of the nonpolar molecules into three-dimensional crystals. It is probable that the molecules of stearic acid cannot prevent the molecules of nonpolar substance from aggromerating into particles of this size but can arrest their further growth into macroscopic particles which would be the case if the molecules of the nonpolar substance exist without the intervening ones of stearic acid. These relations are illustrated schematically in Fig. 3.

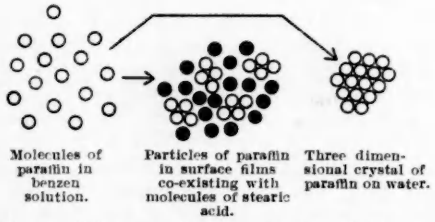
Molecules of paraffin in benzen solution.
Particles of paraffin in surface films co-existing with molecules of stearic acid.
Three dimensional crystal of paraffin on water.

Fig. 3.—Schematical illustration of stabilization of surface film of paraffin by stearic acid: ○ represents a molecule of paraffiin and ● a molecule of stearic acid.

The difference in the size of the particle in the film of the same kind of nonpolar substances will be explained by the difference in the strength of van der Waals force between molecules of the substance. Thus the particle size of paraffin of high melting point is larger than that of low melting point. This is interpreted by the fact that the former is subjected to a stronger van der Waals force between molecules than the latter. But in the other cases the result is often so much complicated that a simple explanation is not applicable. Further it must be noted that the stabilizing action for surface film formation is exhibited not only by stearic acid but also by other acids, alcohols, etc., which form stable monomolecular films on water. The power of these film-stabilizing substances to prevent the molecules of nonpolar substance from aggromerating into three-dimensional crystals will, however, be different from substance to substance, and it will be possible to get some knowledge concerning the nature of various film-stabilizing substances from similar experiments as mentioned above. It must be emphasized that in these cases the special interaction between two substances in mixed films should also be examined if any.

When the film-stabilizing substance is different from stearic acid, the size of the particle stabilized might be expected to be different from that in Table 1. Namely it would depend upon the balance existing between an aggromerating tendency of the nonpolar molecules and an action of the film-stabilizing molecules to prevent them from aggromerating. This property is to be interpreted in relation to the other properties of each substance, which will be discussed later when the further investigation on mixed films is performed.

Summary

It was shown that stable surface films of nonpolar substances could often be formed on water by mixing them with stearic acid, and that in the resulting mixed films the nonpolar substance existed in the state of rather stable unit of particles, forming monoparticle films. The dimension of the surface particles could be calculated for some nonpolar substances. The mechanism of the film-stabilizing action of stearic acid was discussed and it was suggested that the different film-stabilizing substances would stabilize the film of nonopolar substance in a different manner.

In conclusion the author wishes to express his hearty thanks to Prof. Tunetaka Sasaki for his kind guidance in the course of this study.

Department of Chemistry, Faculty of Science, Kyūshū University, Fukuoka

(4) W. D. Harkins, and J. W. Morgan, *Proc. Natl. Acad. Sci.*, **11**, 63 (1925); R. J. Myers and W. D. Harkins, *J. Phys. Chem.*, **40**, 959 (1936).

(5) Ya. B. Aron and Ya. I. Frenkel, *Zhur. Fiz. Khim.* (*J. Phys. Chem.*), **22**, 1243 (1948); *C. A.* **43**, 1240 (1949).

Studies on Monomolecular Films. V. Monomolecular Films of Hardly Spreadable Substances Stabilized by Stearic Acid and Cetyl Alcohol

By Tunetaka SASAKI, Ryôhei MATUURA and Nobumasa FUJIMOTO

(Received June 2, 1951)

In the preceding paper[1] the monoparticle films of nonpolar substances stabilized by stearic acid were discussed. Now it is our problem whether or not a stable monomolecular film on water will be obtained for a substance which is hardly capable of forming a stable monomolecular film by itself, by stabilizing with molecules of fatty acids or alcohols in just the same way as mentioned in the preceding paper. There are many insoluble substances, the molecule of which has polar-nonpolar structure but forms no stable monomolecular films on water due to the lack of balance between polarity and nonpolarity. It is the purpose of the present experiment to prepare stable monomolecular films of some of these substances using stearic acid and cetyl alcohol as stabilizers and to discuss the properties of films thus obtained on the surface of water.

Experimental

Film pressures were measured whith the same apparatus as described already.[2]

All the substances studied in this experiment were purified by recrystallization except for polymer substance such as novolac resin. The substance was mixed with stearic acid or cetyl alcohol in varying proportions and the mixture was dropped as a benzene or benzene~alcohol solution on the surface of water. The pressure~area characteristics were investigated for the resulting surface films.

Results and Discussions

Various insoluble and nonvolatile substances were examined first of all if any monomolecular film is formed by mixing with stearic acid or cetyl alcohol and it was found that there are not so many which form stable monomolecular films on water by this procedure.

The typical example of film stabilization by fatty acid or alcohol are novolac and some azo dye compounds.

(1) Mixed Film of Novolac and Stearic Acid.—The pressure~area diagram of mixed film composed of novolac and stearic acid on $N/100$ hydrochloric acid is shown in Fig. 1.

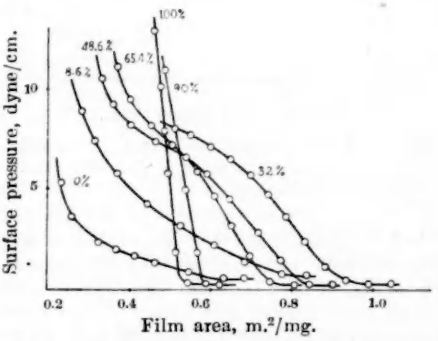

Fig. 1.—Pressure~area diagram of the mixed film composed of novolac and stearic acid on $N/100$ HCl. Percentage refers to stearic acid content.

Novolac does not dissolve in benzene, so alcohol~benzene mixture was used as a solvent for spreading surface film. The surface film of novolac is not stable by itself and its limiting area fluctuates from 0.55 to 0.65 m.²/mg. for each experiment, depending chiefly on the nature of the solvent. But when mixed with stearic acid the film becomes very stable and shows a definite limiting area. The pressure~area curve of the mixed film is similar to that of stearic acid only when the acid content is high and to that of novolac only when it is low. In the intermediate region of acid content there exists a mixed film exhibiting the characteristic pressure~area curve of S-shape.

In Fig. 2 the area composition curve of the mixed film consisting of novolac and stearic acid is shown. The limiting area per mg. of the mixture proves to be in linear relation with the composition of the mixture in the region of the acid content from 100% to 30%.

(1) R. Matuura, This Bulletin, **24**, 200 (1951).
(2) T. Sasaki, *J. Chem. Soc. Japan*, **62**, 796 (1941); R. Matuura and I. Hayasi, *Memoirs of the Faculty of Science, Kyushu University, Ser. C*, Vol. 1, 31 (1948).

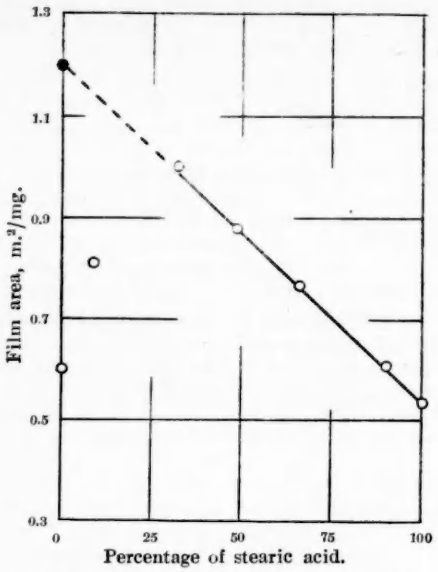

Fig. 2.—Area~composition curve of mixed film composed of novolac and stearic acid on $N/100$ HCl.

This shows presumably, according to the assumption proposed and discussed in the preceding paper,[1] that novolac and stearic acid behave in the mixed film just as if they exist separately. When this linear portion is extrapolated to the zero acid content, the surface area of novolac film without the stabilizing substance is obtained as 1.2m.²/mg. This value is to be taken as the film area of novolac considered to be spread only on the surface of water. On the other hand, as mentioned already, the limiting area of the novolac film which is not stabilized by any film-stabilizing substance fluctuates from 0.55 to 0.65 m.²/mg., about a half of the value expected from the mixed film. This small value might be attributed to the fact that the surface film of novolac is unstable and imperfect unless it is stabilized by a film-stabilizing substance.

The molecule of novolac has more or less a stretched structure and it is reasonable to assume that the chain will lie rather flat on the surface of water. This is explained also by the present experiment on the mixed film which shows that the surface area of novolac is fairly large and the compressibility of the film is much greater than that of stearic acid, as it is usual in the case with surface films of long chain high-molecular substances.[3]

(3) W. D. Harkins, E. F. Carman and H. E. Ries, *J. Chem. Phys.*, **3**, 692 (1935); D. J. Crisp, *J. Colloid Sci.*, **1**, 49, 161 (1946).

(2) Mixed Film of Some Azo Dyes and Cetyl Alcohol.—Film experiments were carried out with some azo dyes using cetyl alcohol as a stabilizer. The molecular structures of the dyes studied are shown in Table 1. These dyes are all incapable of forming stable monomolecular films on the surface of water by themselves. It has been known that some dyes used in this experiment form complex compounds with metallic ions in the bulk reaction. Cetyl alcohol was selected as a stabilizer because it is inert towards metallic ions in the substrate and therefore does not cover the remarkable effect of metallic ions generally encountered for dyes studied.

Pressure~area diagram of the mixed film composed of *p*-toluene-azo-β-naphthol, the compound (I) in Table 1, and cetyl alcohol is shown, as an example, in Fig. 3, where the

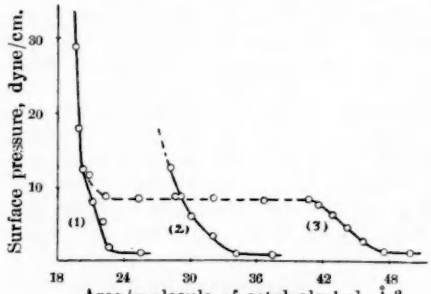

Fig. 3.—Pressure~area curve of mixed film composed of *p*-toluen-azo-β-naphthol and cetyl alcohol on water at pH≒7: (1) monolayer of cetyl alcohol; (2) mixed film of dye and cetyl alcohol (1 : 2); (3) mixed film of dye and cetyl alcohol (1 : 2), water containing 10^{-4} M Cu^{++}/l.

surface area of the mixed film is represented by the area (Å.²) per molecule of cetyl alcohol. The content of the dye is one third in weight of the mixture and the *p*H of the underlying water is about 7. From this figure the limiting area occupied by a molecule of the dye in the mixed film can be calculated as 45.5 Å.² In the same figure the effect of cupric ion is shown. When 10^{-4} mole/liter of cupric ion is present in the underlying water, the area occupied by a molecule of the dye is reduced to 23.5 Å.² This effect is not perceptible when the underlying water is acidic. In the same way we can estimate the area occupied by a molecule in the surface film for the rest of the dyes studied with or without the influence of cupric ion.

Table 1

The Molecular Area of Some Azo Dyes

	Dye	Structural Formula	Molecular area, Å.² on water (pH 7)	Molecular area, Å.² on water containing Cu^{++} (pH 7)
I	*p*-Toluene-azo-*β*-naphthol	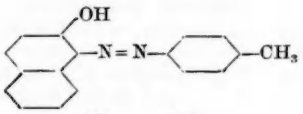	45.5	23.5
II	*o*-Toluene-azo-*β*-naphthol	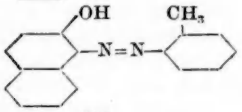	44.7	43.9
III	Benzene-azo-benzene-azo-*β*-naphthol (Sudan III)	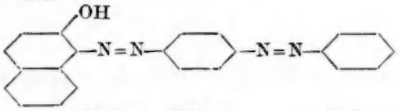	58.5	24.3
IV	*o*-Toluene-azo-*o*-toluene-azo-*β*-naphthol (Sudan IV)	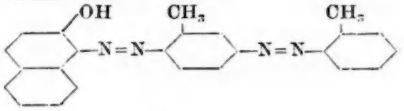	67.6	67.7

The results are shown in Table 1.

Four compounds studied in this experiment have the same molecular structure, in that each has a *β*-naphthol radical at one end while the rest part is rather hydrophobic, although it contains one or two azo groups. It is very much likely that the molecule will be oriented on the surface of water with hydroxyl group of the *β*-naphthol directing to water and the other part to air. The molecule will be bent at the part of azo radical, as is well known in the organic chemistry. From Table 1 it is seen that, although the compounds (I) and (II) have nearly the same molecular area, the molecule of the compound (IV) has larger area than that of the compound (III). This might be due to the existence of methyl groups at the ortho position for azo radical provided that the hydrophobic chain is fairly long.

It is interesting to pay more attention to the effect of metallic ions on them. In Table 1 it is shown that the surface film of the compounds (I) and (III) undergoes a remarkable condensation by the presence of cupric ion, while that of the compounds (II) and (IV) does not. The chief difference of molecular structure worth noticing here between these two groups of the dye compounds consists in that the latter two compounds have a methyl group attached to the ortho carbon atom for azo radical, while the former two have not. If it is assumed that the remarkable condensation of the surface film of the compounds (I) and (III) by cupric ion is attributed to the formation of the complex compounds between the dye molecule in the surface film and cupric ion in the underlying water, it can be presumed that in the case of the compounds (II) and (IV) which are unaffected by cupric ion, the methyl group at the ortho position for azo radical shows hindrance against the formation of such complexes. In fact in a bulk reaction too, it is easy to confirm the formation of a copper complex with the compounds (I) and (III), but very difficult with the compounds (II) and (IV).

The copper complex of the compound (I) is considered to have a chelated structure as follows.

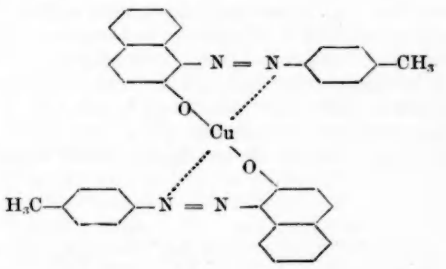

The dye molecule seems to be packed much more compactly with such a complex formation than without. This explains the remarkable condensation of the surface films of the dye compounds (I) and (III) by cupric ion. We can also interpret the further detail of the

pressure~area curves studied, but the precise discussion should be made when more empirical data are available.

Summary

Monomolecular film of novolac and some azo dyes, which are not capable of forming stable monomolecular films by themselves on the surface of water, were prepared using stearic acid or cetyl alcohol as a stabilizer and their properties were measured and discussed. It was shown that the molecule of novolac lies rather flat on the surface of water. The remarkable effect of cupric ion in the underlying water on the dye monolayers was discussed in connection with the molecular structure of the dye compounds.

Department of Chemistry Faculty of Science, Kyûshû University, Fukuoka.

On the Mechanism of Evaporation in Vacuum. I. Evaporation of Silica Gel[1]

By Masayuki NAKAGAKI

(Received June 25, 1951)

The replica methods are usually used to observe the solid surfaces by the electron microscope. Among these, the polystyrene-silica replica method[2],[3],[4] is generally accepted as the method of the best reliability. The cause of the high reliability of silica replica is, as Heidenreich and Peck[2] suggested, due to the high mobility of silica on the polystyrene surface. It is supposed from these facts that silica may evaporate in the form of very low molecular weight, such as a single molecule SiO_2, and deposit and migrate freely on the polystyrene surface, and then polymerize to form a glass-like film. The polystyrene-silica method, however, has some defects. Above all, the evaporation of silica needs a fairly difficult technique. Wyckoff[5] and some others entertained some doubts on the propagation of such a difficult method. Baker and Nicoll[6] tried to obtain the silica film by blowing $SiCl_4$ against the surface of specimen and hydrolysing it on the surface. No satisfactory result was, however, obtained.

The present author used silica gel instead of quartz, and was able to evaporate it very easily. Silica gel was prepared as follows: Dilute commercial water glass to 10 times, add the excess of hydrochloric acid of 1 *N* drop by drop to form jelly, filter by suction, wash with water, adjust it in a rod-like shape, and heat in a crucible. Silica gel was, thus, obtained in a rod shape, the diameter of which was 4 mm. The apparatus used for evaporation was an ordinary one, as shown in Fig. 1. B is a bell jar and G. P. is a rubber packing.

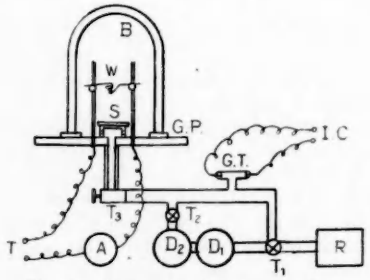

Fig. 1.—Apparatus for evaporation.

Specimen, that is, the polystyrene film, the slide glass, and so forth, are placed at S, and a piece of silica gel is put in the tungsten basket W. A bell jar is evacuated by a rotary pump R and two oil diffusion pumps D_1 and D_2. A tungsten filament W is made of wire

(1) These results were presented before the Meeting of Colloid Chemistry held by the Chemical Society of Japan at Osaka, November 1950.

(2) R. D. Heidenreich and V. G. Peck, *J. Appl. Phys.*, **14**, 23 (1943).

(3) C. H. Gerould, *J. Appl. Phys.*, **18**, 333 (1947).

(4) R. B. Barnes, C. J. Burton and R. G. Scott, *J. Appl. Phys.*, **16**, 730 (1945).

(5) R. W. G. Wyckoff, "Electron Microscopy," New York, 1949, pp. 71 and 93.

(6) R. F. Baker and F. H. Nicoll, *J. Appl. Phys.*, **15**, 803 (1944).

of 0.5 mm. in diameter, which is coiled about 6 times in corn of 8 mm. in hight and 30° in the vertical angle. Various voltages are applied on the filament by a transformer T and current is read by the ammeter A. G.T. is a Geisler's tube and I. C. is an induction coil, by which vacuum in the bell jar is known.

Heating silica gel in a crucible does not seem to be sufficient to dehydrate it. By a rapid evaporation of water contained in the gel, it bursts and splashes, if much current is hastily applied. In order to avoid such trouble, and to keep vacuum in the bell jar better, preheating of the filament for 15 or 30 sec., with 150 watts or so, is desirable. Some examples of data are shown in Table 1. In this table, w_0

Table 1

Evaporation of Silica Gel

Exper. No.	w_0, mg.	V, volt	A, amp.	t, sec.	W, watt	Wt/w_0
1	4	10	14	15	140	(preheating)
		15	18	20	270	= 1350
2	6	10	15	60	150	(preheating)
		13	18	30	234	= 1170
3	8	10	20	15	200	(preheating)
		15	24	30	360	= 1350
4	8	8	12.5	180	100	(preheating)
		15	17	30	255	
		17	18	10	306	= 1339
5	18	5	10	15	50	
		10	14.5	15	145	(preheating)
		13	17	60	221	
		15	18	30	270	= 1186
6	20	5	10	15	50	
		10	13	30	130	(preheating)
		15	18	110	270	= 1485

is the weight of silica gel evaporated, V and A are voltage and current applied to the tungsten basket, respectively, t is the time in which current is closed, W is the product of V and A, that is the power supplied, and Wt/w_0 corresponds to the energy provided for the evaporation of 1 mg. of silica gel. The most part of this energy is emitted away as radiation, and only a very small part of it is used to evaporate the gel. Wt/w_0 may have, therefore, no theoretical meaning. If the experiments are done, however, under a definite condition, Wt/w_0 may be used as a practical measure of the easiness of evaporation. From Table 1, it is seen that

$$Wt/w_0 = 1{,}000 \sim 1{,}500 \text{ joule/mg.}$$

In the case of quartz, data of Heidenreich and Peck[2] and Gerould[3] shows that

$$Wt/w_0 = 3{,}800 \sim 14{,}000 \text{ joule/mg.}$$

which is 3~9 times greater than the value for silica gel. It is recognized from these values that silica gel evaporates much more easily than quartz. It is experienced that silica gel evaporats as easily as chromium.

Polystyrene silica replica is made as follows. Polystyrene replica is made by the low pressure method or the lacquer method. In the low pressure method, 1 cm.^{2} of the polystyrene film, 0.02 mm. in thickness, is placed on a slide glass, and heated on a metal plate to 150~200°C. The specimen, another silde glass, and a weight of 1 kg. are put on the film and cooled below 80°. Specimen is splitted from the film, and silica gel is evaporated on the film according to the method described above. In the lacquer method, one drop of polystyrene lacquer, that contains 1 g. of polystyrene in 15 cc. of benzene, is placed on the specimen and dried. The replica film is stripped after 2 days, and placed on a slide glass and silica is evaporated to it. The thickness of silica film deposited is calculated by the equation:

$$d = \frac{h\ w_0}{4\pi\ (h^2+r^2)^{3/2}\ \rho} \qquad (1)$$

where h is the height of tungsten basket above the polystyrene replica, 6~7 cm., r is the horizontal distance of the basket from the film, 4~5 cm., and w_0 is the weight of silica gel used, 4~5 mg. ρ is the density of silica film. A reliable value of ρ is not known. The value of bulk quartz $\rho=2.22$ is used. The thickness calculated was usually 200~300 Å. Williams and Backus[7] asserted that the value of d of equation (1) should be multiplied by an "efficiency factor" 3/4. The foundation of their opinion is somewhat uncertain, and a preliminary experiment by the present author to determine the thickness of the silica film directly from the interference color for somewhat thicker one seemed to show that such a factor is rather unnecessary. No efficiency factor is, therefore, used. The polystyrene-silica replica film thus obtained is cut off in pieces of 3~5 mm. square. One of the pieces is pasted on a holder for the electron microscopy, facing the silica surface downward and the polystyrene surface upward. The difficulty of "Fishing" is thus avoided. Paste used must be insoluble in benzene. Usual starch paste is available. These holders are laid in benzene for 1~2 days and put out carefully, holding the replica film vertically, from benzene and laid on a filter paper and dried. Some electron micrographs obtained are shown in Fig. 2. (a) is the surface

(7) R. C. Williams and R. C. Backus, *J. Appl. Phys.*, **20**, 98 (1949).

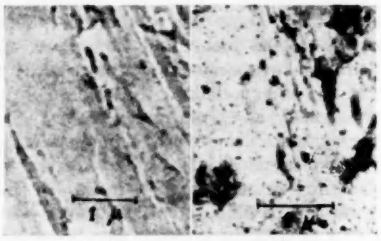

(a) (b)

Fig. 2. — Electron micrograph.

of a brass polished by sandpaper. The lacquer method is used and silica film is 250 Å. thick. (b) is the surface of a carbon brush. The low pressure method and silica film of 200 Å. are used. Reliability of these replica method is not yet tested, but, at least, the granular structure of silica film is not found. In Fig. 2 the applicability of this replica method for electron micrography are shown.

In order to comprehend the easiness of the evaporation of silica gel, it is necessary to know the vapor pressure of it. The estimation of vapor pressure is tried. Clapeyron-Clausius' equation, usually used to describe the vapor pressure curve, is written under some approximation as:

$$\frac{\mathrm{d}\ln P}{\mathrm{d}T} = \frac{L}{RT^2}, \qquad (2)$$

where P is vapor pressure, T is absolute temperature, R is gas constant, and L is heat of sublimation or evaporation. Using Nernst's assumption:

$$L = L_0 + 1.5\,T - \varepsilon T^2 + RT \qquad (3)$$

Eq (1) is integrated to

$$\log P(\mathrm{atm.}) = -L_0/2.303\,RT + 1.75\log T - \varepsilon T/2.303\,R + \kappa, \qquad (4)$$

where P(atm.) is the pressure expressed in atmosphere, and κ is the conventional chemical constant and ε is a parameter determined from experimental data, *e. g.*, boiling point.

It is known[8] that the boiling point, Tv, of rock crystal or quartz is 2590°. It is assumed that silica evaporates as SiO_2, which is thought to be a linear molecule. The conventional chemical constant[9] κ is, then,

$$\kappa = -3.273 + 1.5\log M + \log(N_A A \times 10^{16}) \qquad (5)$$

where M is molecular weight, 60.06, N_A is Avogadro's number, and A is the moment of inertia of the molecule. Assuming the Si=O distance to be 1.62 Å., the value of κ of Eq. (5) is obtained as 1.319. If the value of L_0 is obtained, vapor pressure P is calculated from Eq. (4), with the estimated value of ε by the use of T_v.

The heat of sublimation of quartz $L_0^{(A)}$ is approximately equal to twice the bond energy of Si-O,

$$L_0^{(A)} \simeq 2D(\mathrm{Si\text{-}O}) \qquad (6)$$

This is easily seen from Fig. 3 (a), because four bonds should be broken to produce a molecule of SiO_2, and each bond is held in

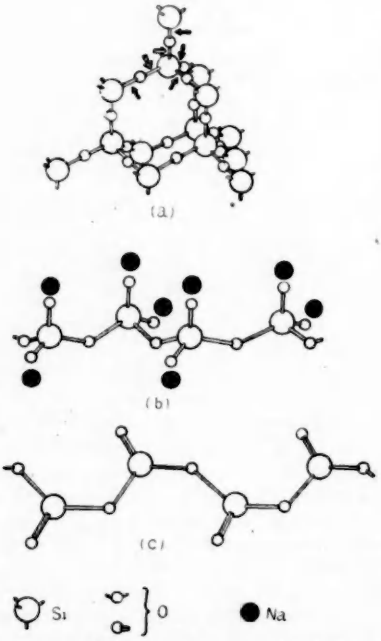

Fig. 3.—Molecular structure of silica.

common with two SiO_2 molecules. The bond energy D(Si-O) is calculated by Pauling[10] from the data of the heat of generation of quartz as:

$$D(\mathrm{Si\text{-}O}) = 89.3\ \mathrm{kcal./mol.} \qquad (7)$$

Seitz[11] cited the cohesive energy of quartz E as

(8) Edited by Tokyo Astronomical Observatory, "Rika-Nenpyo", Tokyo, 1950.

(9) R. H. Fowler and E. A. Guggenheim, "Statistical Thermodynamics", Cambridge, 1939, p. 171.

(10) L. Pauling, "The Nature of the Chemical Bond," New York, 1940, p. 53.

(11) F. Seitz, "The Modern Theory of Solid", New York, 1940, p. 61.

$$E = 405.7 \text{ kcal./mol.} \quad (8)$$

E is the energy necessary to produce one gram atom of Si and two gram atom of O from quartz, and equals to the sum of $L_0^{(A)}$ and $2D(\text{Si-O})$, as shown in Fig. 3 (a). Therefore,

$$E \simeq L_0^{(A)} + 2D(\text{Si-O}) \simeq 4D(\text{Si-O}) \quad (9)$$

From Eqs. (8) and (9),

$$D(\text{Si-O}) \simeq 101.4 \text{ kcal./mol.} \quad (10)$$

This is the same order of magnitude with Pauling's value, Eq. (7), but is not exactly equal. The mean value

$$D(\text{Si-O}) = 95.4 \text{ kcal./mol.} \quad (11)$$

is used in the following estimations. From Eq. (6),

$$L_0^{(A)} = 190.8 \text{ kcal./mol.} \quad (12)$$

Silica gel is prepared from water glass, $(Na_2SiO_3)_n$, which is considered as a chain polymer as shown in Fig. 3 (b). The idealized structure of silica gel, therefore, will be also a chain polymer. The heat of sublimation of idealized silica gel, $L_0^{(B)}$, will be, as explained easily from Fig. 3 (c),

$$L_0^{(B)} \simeq D(\text{Si-O}) = 95.4 \text{ kcal./mol.} \quad (13)$$

As for actual silica gel, the probability of dehydration from two hydroxyl groups of adjacent molecules forming an oxygen bridge should be taken into account, beside with the probability of dehydration from two hydroxyl groups belonging to the same silica atom in meta-silicic acid molecule. Under the somewhat arbitrary assumption that the latter probability is twice as large as the former probability, the heat of sublimation of real silica gel $L_0^{(C)}$ becomes:

$$L_0^{(C)} = \frac{2L_0^{(B)} + L_0^{(A)}}{3} = \frac{4}{3} D(\text{Si-O})$$
$$= 127.2 \text{ kcal./mol.} \quad (14)$$

Using these values of the heat of sublimation L_0, vapor pressure is calculated for various temperatures, using $\kappa = 1.319$ and $\varepsilon = -0.01145$, the latter is obtained from boiling point for quartz. For some metals, vapor pressure curves are estimated in an analogous way, and temperature corresponding to some vapor pressure are cited in Table 2. In this table, SiO_2(A) means

Table 2

Calculated Vapor Pressure—Temperature Relations

Substances	Temperature corresponding to the vapor pressure, °K.			
	10 mm.Hg	10^{-1} mm.Hg	10^{-3} mm.Hg	10^{-5} mm.Hg
Pt	3300	2600	2200	1900
SiO_2 (A)	2650	2450	2250	2050
Au	2200	1850	1550	1350
SiO_2 (C)	2000	1800	1650	1500
Cr	2050	1750	1500	1300
SiO_2 (B)	1650	1450	1300	1150
Al	1700	1400	1200	1050

quartz, SiO_2 (B) means idealized silica gel and SiO_2 (C) means actual silica gel. It is seen that the evaporation of quartz is almost as difficult as platinum, while silica gel, SiO_2 (C), evaporates as easily as gold or chromium. These agree well with the results described above.

Summary

The evaporation of silica is facillitated by the use of silica gel, instead of quartz. The silica film thus obtained is available as replica for the electron microscopy. The difference of the easiness of evaporation between quartz and silica gel is atributed to molecular constitutions. Under the assumption that quartz consists of three dimensional net work of covalent linkage, while silica gel is constructed by linear chain having some oxygen bridges between chains, vapor pressure is calculated, and the ease of evaporation is accounted for by the comparison to some usual metals.

Thanks are due to Mr. S. Okada for his kind help to the operation of the electron microscope.

Chemical Institute, Faculty of Science the University of Tokyo, Tokyo.

LETTER

Electrophoresis of Desoxypentose Nucleic Acids Treated with Acid and Alkali

By Nobuo UI and Itaru WATANABE

(Received September 15, 1951)

Recently, some physico-chemical studies of the effect of acids and bases on the macromolecular properties of desoxypentose nucleic acid (DNA) have been carried out by several investigators.[1]

During the electrophoretic studies on nucleic acids[2] now in progress, the present authors have found an appreciable variation of the mobility of DNA after the treatment with alkali as well as acid. The acid-treatment also causes a change in the electrophoretic pattern.

DNA was prepared from herring sperm or calf thymus by the modified Hammarsten's method and dissolved in water. A neutral solution was brought to *p*H 12.0 by adding sodium hydroxide and immediately neutralised again directly with hydrochloric acid or by dialyzing against the phosphate buffer of *p*H 7.7 In both cases, only one homogeneous component was found, as in the case of native DNA, when examined by electrophoresis in phosphate buffer (*p*H 7.7, ionic strength 0.2) using a Tiselius-type apparatus. The mobility of the alkali-treated samples, however, was considerably lower than that of the untreated DNA, while Creeth *et al.*[3] reported the absence of any difference between the mobilities of both treated and untreated samples in the wide *p*H range. Representative results are shown in Table 1, together with the mobility of the sample which had been boiled in an alkaline solution for one hour and precipitated with HCl-containing ethanol. It is rather curious that the mobility of this alkali-boiled DNA is still larger than that of yeast nucleic acid (YNA), the latter being *ca.* -14×10^{-5} cm²/sec. volt, though those two nucleic acids have similar molecular size and shape.[4] This result also differs from Cohen's data[5] that Leven's DNA migrates with the same mobility as YNA.

Table 1

Electrophoretic Mobilities of Alkali-treated DNA at 0°C. (In phosphate buffer of *p*H 7.7 and ionic strength 0.2)

Samples	Mobilities (calcd. from descending pattern), $\times10^5$ cm²/sec. volt
(a) Untreated DNA	−16.0
(b) Alkali-treated DNA	−15.0
(c) (a) + (b)	−15.2, −16.4
(d) Alkali-boiled DNA	−15.5
(e) (d) + YNA	−15.3, −13.9*

* The mobility of YNA.

On the other hand, somewhat different phenomena have been observed after the acid treatment. For example, the sample, once brought to *p*H 3.0 and immediately neutralised again, showed a slightly inhomogeneous pattern indicating the presence of a small amount of faster component. When kept at *p*H 3.0 for 48 hours before the neutralisation, this faster component became more distinct. In both cases, the mobility of the main (slower) component was exactly the same as that of the alkali-treated DNA.

Details of this work will be published elsewhere with the discussion on the possible explanations for these experimental results.

Institute of Science and Technology
University of Tokyo, Tokyo

(1) C. F. Vilbrandt and H. G. Tennent, *J. Am. Chem. Soc.*, **65**, 1866 (1943); J. M. Gulland, D. O. Jordan and H. F. W. Taylor, *J. Chem. Soc.*, **1947**, 1131; J. M. Creeth, J. M. Gulland and D. O. Jordan, *ibid.*, **1947**, 1141; R. Cecil and A. G. Ogston, *ibid.*, **1948**, 1382; I. Jungner, *Acta physiol. Scand.*, **20**, Suppl. 69 (1950); S. Zamenhof and E. Chargaff, *J. Biol. Chem.*, **186**, 207 (1950).

(2) I. Watanabe and N. Ui, *Repts. Radiation Chem. Research., Inst., Tokyo Univ.*, **5**, 17 (1950).

(3) J. M. Creeth, D. O. Jordan and J. M. Gulland, *J. Chem. Soc.*, **1949**, 1406.

(4) I. Watanabe and T. Kitamura, unpublished data.

(5) S. S. Cohen, *J. Biol. Chem.*, **146**, 471 (1942).

No. 4

ated
I 7.7

l. from
tern),
volt

16.4

13.9*

n Table
which
on for
taining
obility
r than
latter
though
lecular
rs from
igrates

ifferent
e acid
, once
ralised
pattern
unt of
.0 for
faster
both
com-
of the

l else-
ossible
lts.

ology